

Polytopes, lattices, and spherical codes for the nearest neighbor problem

Thijs Laarhoven¹

TU/e, The Netherlands
mail@thijs.com

Abstract. We study locality-sensitive hash methods for the nearest neighbor problem for the angular distance, focusing on the approach of first projecting down onto a low-dimensional subspace, and then partitioning the projected vectors according to Voronoi cells induced by a suitable spherical code. This approach generalizes and interpolates between the fast but suboptimal hyperplane hashing of Charikar [STOC 2002] and the asymptotically optimal but practically often slower hash families of e.g. Andoni–Indyk [FOCS 2006], Andoni–Indyk–Nguyen–Razenshteyn [SODA 2014] and Andoni–Indyk–Laarhoven–Razenshteyn–Schmidt [NIPS 2015]. We set up a framework for analyzing the performance of any spherical code in this context, and we provide results for various codes from the literature, such as those related to regular polytopes and root lattices. Similar to hyperplane hashing, and unlike e.g. cross-polytope hashing, our analysis of collision probabilities and query exponents is *exact* and does not hide order terms which vanish only for large d , thus facilitating an easy parameter selection. For the two-dimensional case, we analytically derive closed-form expressions for arbitrary spherical codes, and we show that the equilateral triangle is optimal, achieving a better performance than the two-dimensional analogues of hyperplane and cross-polytope hashing. In three and four dimensions, we numerically find that the tetrahedron and 5-cell (the 3-simplex and 4-simplex) and the 16-cell (the 4-orthoplex) achieve the best query exponents, while in five or more dimensions orthoplices appear to outperform regular simplices, as well as the root lattice families A_k and D_k . We argue that in higher dimensions, larger spherical codes will likely exist which will outperform orthoplices in theory, and we argue why using the D_k root lattices will likely lead to better results in practice, due to a better trade-off between the asymptotic query exponent and the concrete costs of hashing.

Keywords: (approximate) nearest neighbor problem, spherical codes, polytopes, lattices

1 Introduction

Given a large database of high-dimensional vectors, together with a target data point not in the database, a natural question to ask is: which item in the database is the most similar to the query? And can we somehow preprocess and store the database in a data structure that allows such queries to be answered faster? These and related questions have long been studied in various contexts, such as machine learning, coding theory, pattern recognition, and cryptography [DHS00, SDI05, Bis06, Dub10, Laa15, MO15], under the headers of *similarity search* and *nearest neighbor searching*.

Depending on the context of the problem, different solutions for these problems have been proposed and studied. In the late 1990s, Indyk–Motwani [IM98] proposed the *locality-sensitive hashing* framework, and until today this method remains one of the most prominent and popular methods for nearest neighbor searching in high-dimensional vector spaces, both due to its asymptotic performance when using theoretically optimal hash families [AINR14, AIL⁺15], and due to its practical performance when instantiated with truly efficient locality-sensitive hash functions [Ach01, Cha02, Ber16]. And whereas many other methods fail as the dimensionality of the problem increases, locality-sensitive hashing remains competitive even in high-dimensional settings.

Although solutions for both asymptotic and concrete settings have been studied over the years, there is often a separation between both cases: some methods work well in practice, but do not scale optimally when the parameters increase (e.g. [Cha02]); while other methods are known to

achieve a superior performance for sufficiently large parameter sizes, but are not quite as practical in most applications due to large hidden order terms in the asymptotic analysis (e.g. [AI06, AINR14, AIL⁺15, BDGL16, ALRW17]). Moreover, the latter methods are not as easy to deploy in practice due to these unspecified hidden order terms, making it hard to choose parameters accurately. A key problem in this area thus remains to close the gap between theory and practice, and to offer solutions that interpolate between *quick-and-dirty* simple approaches, and more sophisticated methods that start outperforming these simpler methods as the parameters increase.

1.1 Related work

In this paper we focus on methods for solving the nearest neighbor problem for the *angular distance*, which is closely related to the nearest neighbor problem in various ℓ_p -norms: as demonstrated by Andoni–Razenshteyn [AR15], a solution for the nearest neighbor problem for the angular distance (or for the Euclidean distance on the unit sphere) can be optimally extended to a solution for all of \mathbb{R}^d for the Hamming and Euclidean distances through a somewhat efficient reduction.

For the angular distance, perhaps the most well-known and widely deployed approach for finding similar items in a database is to use the hyperplane hash family of Charikar [Cha02]. For spherically-symmetric, random data sets on the sphere of size n , it can find a nearest neighbor at angle at most $\theta = \frac{\pi}{3}$ in sublinear time $O(n^\rho)$ and space $O(n^{1+\rho})$, with $\rho \approx 0.5850$. Various improvements later showed that smaller values ρ can be achieved in sufficiently high dimensions [AI06, AINR14], the most practical of which is based on cross-polytopes or orthoplices [TT07, AIL⁺15, KW17]: for large d and target angle $\theta = \frac{\pi}{3}$, the query time complexity scales as $n^{\rho+o(1)}$ with $\rho = 1/3$. The convergence to the limit however is very slow [AIL⁺15, Theorem 1] and depends on both d and n being large. In practical applications, hyperplane hashing often still dominates [MLB15, MLB17, Ber16].

Related to the topic of this paper, various papers have further observed the relation between finding good locality-sensitive hash families and finding nice spherical codes that partition the sphere well, and allow for efficient decoding [AI06, TT07, TT09, AIL⁺15, CDGG18]. The requirements on a spherical code to be a *good* spherical code are somewhat intricate to state, and to date it is an open problem to exactly quantify which spherical codes are the most suited for nearest neighbor searching. It may well be possible to improve upon the state-of-the-art orthoplex (cross-polytope) locality-sensitive hashing [AIL⁺15, RS16] in practice with a method achieving the same (optimal) asymptotic scaling, but with a faster convergence to the limit.

1.2 Contributions

In this paper we provide a framework for analyzing the performance of spherical codes in the context of locality-sensitive hashing for the angular distance, relating the collision probabilities appearing in the analysis of these hash functions to so-called *orthant probabilities* of multivariate normal distributions with non-trivial correlation matrices. Below we state this relation for general spherical codes, providing a recipe for computing the collision probabilities as a function of the set of vertices \mathcal{C} of the corresponding spherical code.

Theorem 1 (Spherical code locality-sensitive hashing – Restatement of Theorem 8).

Let $\mathcal{C} = \{\mathbf{c}_1, \dots, \mathbf{c}_c\} \subset \mathcal{S}^{k-1}$ be a k -dimensional spherical code of size c , and for $i = 1, \dots, c$, let $\mathbf{C}_i \in \mathbb{R}^{k \times k}$ denote the matrix whose j^{th} row is the vector $\mathbf{c}_i - \mathbf{c}_j$. Let \mathcal{H} consist of functions $h = h_{\mathbf{A}}$ of the form $h(\mathbf{x}) = \text{dec}(\mathbf{A}\mathbf{x}) \in \{1, \dots, c\}$, with $\mathbf{A} \sim \mathcal{N}(0, 1)^{k \times d}$, and $\text{dec}(\cdot)$ representing decoding to the nearest code word in \mathcal{C} . Then for any $\theta \in (0, \frac{\pi}{2})$, \mathcal{H} is a (θ, p_1, p_2) -sensitive hash family, with:

$$p_1 = \sum_{i=1}^c \Pr_{\mathbf{z} \sim \mathcal{N}(\mathbf{0}, \Sigma_i)}(\mathbf{z} \geq \mathbf{0}), \quad \Sigma_i = \begin{bmatrix} 1 & \cos \theta \\ \cos \theta & 1 \end{bmatrix} \otimes (\mathbf{C}_i \mathbf{C}_i^T), \quad p_2 = \frac{1}{\mu(\mathcal{S}^{d-1})^2} \sum_{i=1}^c \mu(\mathcal{V}_i)^2. \quad (1)$$

Above, \mathcal{H} being (θ, p_1, p_2) -sensitive means that random vectors collide with probability at most p_2 , and target nearest neighbors at angle at most θ from a random query vector collide in a random hash function $h \sim \mathcal{H}$ with probability at least p_1 . The folklore locality-sensitive hashing exponent $\rho = \log p_1 / \log p_2$ then describes the distinguishing power of this hash family, as for large n this tells us we can solve the (average-case) nearest neighbor problem with angle θ with query time $\tilde{O}(n^\rho)$.

We show how to explicitly compute the correlation matrices Σ appearing in the theorem above, how to reduce the dimensionality of the problem (and of the matrices \mathbf{C}_i above) using only the *relevant vectors* of each code word, and how the analysis can be further simplified when the spherical code exhibits many symmetries, such as being isogonal.

Using this framework, we first rederive the celebrated result of Charikar [Cha02] for one-dimensional spherical codes, noting that the collision probability analysis dates back to a result from the late 1800s [She99]. Applying the same framework to two-dimensional codes, we establish that *triangular locality-sensitive hashing* achieves a superior performance to hyperplane hashing.

Theorem 2 (Triangular locality-sensitive hashing). *Let $\mathbf{x}, \mathbf{y} \in \mathbb{R}^d$, and let $\phi(\mathbf{x}, \mathbf{y})$ denote their mutual angle. Consider hash functions $h : \mathbf{u} \mapsto \text{dec}(\mathbf{A}\mathbf{u})$, with $\mathbf{A} \sim \mathcal{N}(0, 1)^{2 \times d}$, and where $\text{dec} : \mathbb{R}^2 \rightarrow \{1, 2, 3\}$ decodes to the index of the nearest vertex from an equilateral triangle centered at the origin. Then:*

$$\Pr_{\mathbf{A} \sim \mathcal{N}(0, 1)^{2 \times d}} \left(h(\mathbf{x}) = h(\mathbf{y}) \mid \phi(\mathbf{x}, \mathbf{y}) = \theta \right) = \frac{1}{3} + 3 \left(\frac{\pi - \theta}{2\pi} \right)^2 - 3 \left(\frac{\arccos(\frac{1}{2} \cos \theta)}{2\pi} \right)^2. \quad (2)$$

We stress that the collision probability above is *exact*, and does not hide any order terms in d .¹ For random data sets, this implies that with this hash family we can find neighbors at angle at most $\frac{\pi}{3}$ in time $O(n^\rho)$ with $\rho \approx 0.56996$, offering a concrete improvement over the hyperplane hashing approach of Charikar [Cha02] with query exponent $\rho \approx 0.5850$. We further establish that this is the best we can do with any two-dimensional isogonal spherical code, and we numerically estimate that this code achieves the lowest values ρ among all two-dimensional spherical codes.

For three-dimensional codes, through numerical integration of the resulting orthant probabilities, we conclude that the *tetrahedron* seems to minimize the query exponent ρ out of all three-dimensional codes, beating the three-dimensional analogues of the cross-polytope and hypercube, as well as various sphere packings and other regular polytopes, such as the Platonic and Archimedean solids. In four dimensions an interesting phenomenon occurs: the *5-cell* (4-simplex) and *16-cell* (4-orthoplex) are optimal in different regimes, with the 5-cell inducing a more coarse-grained partition of the space and achieving a better performance when the nearest neighbor lies relatively far away, and the 16-cell inducing a more fine-grained partition, and working better when the nearest neighbor lies close to the target vector. This strengthens our intuition that, as the dimensionality goes up, or as the nearest neighbor lies closer to the target vector, more fine-grained partitions generated by larger spherical codes are needed to obtain the best performance.

For higher-dimensional codes, we obtain further improvements in the query exponents ρ through the use of suitable spherical codes, as shown in Table 1 and Figures 1 and 2. For dimensions 5 and 6, the corresponding orthoplices achieve a better performance than the simplices. By estimating values ρ obtained by *utopian* spherical codes, where each cell corresponds to a perfect spherical cap, and optimizing over the number of cells, we predict that the optimal code size increases faster than the linear scaling given by simplices and orthoplices. In higher dimensions, we predict that more suitable spherical codes exist, achieving lower values ρ than the orthoplices. Finding such spherical codes is likely to be closely related to other sphere packing problems.

¹ In fact, the collision probabilities do not depend on d at all, due to our choice of \mathbf{A} being Gaussian.

1.3 Practical aspects

Although the exponent ρ , and therefore the probabilities p_1 and p_2 , directly imply the main performance parameters to assess the asymptotic performance of a locality-sensitive hash family, in practice we are always dealing with concrete, non-asymptotic values n , d , and θ – if the convergence to the optimal asymptotic scaling is slow, or if the hash functions are expensive to evaluate in practice, then hash families with lower query exponents ρ may actually be less practical for small, concrete values of n and d than fast hash families such as hyperplane hashing. In practice one therefore needs to find a balance between asymptotic and concrete aspects of a hashing scheme.

For instance, whereas hyperplane hashing [Cha02] allows us to partition a sphere in 2^k regions with a single random projection matrix $\mathbf{A} \in \mathbb{R}^{k \times d}$ (or equivalently k matrices $\mathbf{A}_1, \dots, \mathbf{A}_k \in \mathbb{R}^{1 \times d}$ merged into one large matrix), for cross-polytope hashing [AIL⁺15] a k -dimensional projection would only divide the sphere into $2k$ regions. As the required number of hash buckets is often roughly the same, regardless of the chosen hash family,² this means that if we wish to divide the sphere into 2^k hash regions with cross-polytope hashing, we would need $m = k / \log_2(2k)$ independent random projection matrices $\mathbf{A}_1, \dots, \mathbf{A}_m \in \mathbb{R}^{k \times d}$ to hash a vector to one of 2^k buckets. So even though the resulting partitions for cross-polytope hashing might generate smaller exponents ρ , in practice this improvement may not offset the additional costs of computing the projections/rotations, which is almost a linear factor $O(d)$ more than for hyperplane hashing.

We explicitly quantify the trade-off between the complexity of the hash functions and the asymptotic query exponents ρ in Figure 3, where on the vertical axis we plotted the query exponents ρ as computed in this paper, and on the horizontal axis we plotted the number of bits extracted per row of a projection matrix; for hyperplane hashing we extract 1 bit per projection, while e.g. for cross-polytope hashing in dimension k we only extract $\log(2k)/k$ bits per projection. Depending on the application, it may be desirable to choose hash families with slightly larger values ρ , if this means the cost of the hashing becomes less. Figure 3 makes a case for using hashes induced by the root lattices D_k , as well as those induced by exotic polytopes such as the 2_{21} -polytope; compared to e.g. the 5-orthoplex, the D_{10} lattice achieves lower values ρ and extracts more bits per projection, while the 2_{21} -polytope further improves upon D_{10} by extracting more hash bits per projection.

To further illustrate how these trade-offs might look in a practical setting, Figure 4 describes a case study for average-case nearest neighbor searching with different sizes n for the data sets. For small data sets, hyperplane hashing is quite competitive, and the best other spherical codes are those induced by the D_k lattices (for small k), and spherical codes generated by the polytopes 1_{21} , 1_{31} and 2_{21} . This case study matches the recommendations from Figure 3. For large n , the role of ρ becomes more prominent, and higher-dimensional orthoplices and D_k lattices give the best performances. In Section 10 we further discuss how one might choose the best codes in practice.

1.4 Outline

In Section 2 we describe preliminary results and notation. Section 3 defines the model for the nearest neighbor problem, and how to analyze the project-and-partition approach for arbitrary spherical codes. Sections 4–7 continue with applying this framework to spherical codes in dimensions 1 through 4, and Section 8 describes results for spherical codes in higher dimensions. Section 9 continues with (conjectured) lower bounds on the parameter ρ in this framework, based on the performance of a utopian spherical code consisting of disjoint spherical caps. Section 10 continues with a more practical analysis, and Section 11 concludes with a discussion of the results.

² While a hash family with lower query exponents ρ does require a smaller number of hash buckets per hash table, this effect is marginal compared to the increase in the number of projections/rotations required by e.g. cross-polytope hashing compared to hyperplane hashing.

k	spherical code	c	I?	$ \mathcal{R} $	$\rho(\frac{\pi}{12})$	$\rho(\frac{\pi}{6})$	$\rho(\frac{\pi}{4})$	$\rho(\frac{\pi}{3})$	$\rho(\frac{5\pi}{12})$
1	spherical caps				$0.1255^{(2)}$	$0.2630^{(2)}$	$0.4150^{(2)}$	$0.5850^{(2)}$	$0.7776^{(2)}$
	hyperplane	2	Y	1	0.1255	0.2630	0.4150	0.5850	0.7776
2	spherical caps				$0.1194^{(3)}$	$0.2518^{(3)}$	$0.4005^{(3)}$	$0.5700^{(3)}$	$0.7666^{(3)}$
	triangle (S_2)	3	Y	2	0.1194	0.2518	0.4005	0.5700	0.7666
	square (O_2, C_2, D_2)	4	Y	2	0.1255	0.2630	0.4150	0.5850	0.7776
	pentagon	5	Y	2	0.1343	0.2788	0.4346	0.6040	0.7905
	hexagon (A_2)	6	Y	2	0.1438	0.2954	0.4544	0.6222	0.8022
3	spherical caps				$0.1117^{(5)}$	$0.2389^{(4)}$	$0.3846^{(4)}$	$0.5548^{(4)}$	$0.7561^{(4)}$
	tetrahedron (S_3)	4	Y	3	0.1155	0.2445	0.3910	0.5600	0.7592
	sphere packing	5	N	-	0.1170	0.2481	0.3965	0.5664	0.7644
	octahedron (O_3)	6	Y	4	0.1159	0.2465	0.3952	0.5661	0.7649
	sphere packing	7	N	-	0.1207	0.2554	0.4065	0.5772	0.7725
	cube (C_3)	8	Y	3	0.1255	0.2630	0.4150	0.5850	0.7776
	sphere packing	9	N	-	0.1217	0.2591	0.4129	0.5850	0.7786
	icosahedron	12	Y	5	0.1255	0.2678	0.4255	0.5983	0.7883
	cuboctahedron (A_3, D_3)	12	Y	4	0.1294	0.2728	0.4301	0.6017	0.7900
	dodecahedron	20	Y	3	0.1509	0.3077	0.4692	0.6360	0.8112
4	spherical caps				$0.1050^{(7)}$	$0.2285^{(6)}$	$0.3730^{(6)}$	$0.5433^{(5)}$	$0.7466^{(5)}$
	5-cell (S_4)	5	Y	4	0.1126	0.2392	0.3840	0.5527	0.7537
	sphere packing	6	N	-	0.1128	0.2401	0.3861	0.5555	0.7564
	sphere packing	7	N	-	0.1120	0.2392	0.3852	0.5553	0.7567
	16-cell (O_4)	8	Y	6	0.1107	0.2368	0.3822	0.5528	0.7553
	sphere packing	10	N	-	0.1136	0.2426	0.3909	0.5623	0.7622
	sphere packing	13	N	-	0.1133	0.2439	0.3939	0.5666	0.7663
	tesseract (C_4)	16	Y	4	0.1255	0.2630	0.4150	0.5850	0.7776
	runcinated 5-cell (A_4)	20	Y	6	0.1216	0.2586	0.4128	0.5855	0.7795
octacube (D_4)	24	Y	8	0.1202	0.2577	0.4140	0.5877	0.7823	
5	spherical caps				$0.0997^{(13)}$	$0.2203^{(10)}$	$0.3630^{(8)}$	$0.5342^{(7)}$	$0.7415^{(6)}$
	5-simplex (S_5)	6	Y	5	0.1105	0.2354	0.3785	0.5469	0.7493
	5-orthoplex (O_5)	10	Y	8	0.1076	0.2299	0.3733	0.5433	0.7483
	1 ₂₁ -polytope	16	Y	10	0.1080	0.2330	0.3794	0.5516	0.7554
	expanded 5-simplex (A_5)	30	Y	8	0.1167	0.2494	0.4007	0.5735	0.7713
	5-hypercube (C_5)	32	Y	5	0.1255	0.2630	0.4150	0.5850	0.7776
rectified 5-orthoplex (D_5)	40	Y	12	0.1139	0.2471	0.4009	0.5757	0.7739	
6	spherical caps				$0.0955^{(18)}$	$0.2135^{(15)}$	$0.3552^{(11)}$	$0.5263^{(9)}$	$0.7357^{(8)}$
	6-simplex (S_6)	7	Y	6	0.1089	0.2319	0.3742	0.5422	0.7458
	6-orthoplex (O_6)	12	Y	10	0.1065	0.2260	0.3670	0.5361	0.7431
	2 ₂₁ -polytope	27	Y	16	0.1038	0.2258	0.3712	0.5442	0.7510
	1 ₃₁ -polytope	32	Y	15	0.1062	0.2314	0.3788	0.5520	0.7564
	expanded 6-simplex (A_6)	42	Y	10	0.1133	0.2427	0.3917	0.5642	0.7647
	rectified 6-orthoplex (D_6)	60	Y	16	0.1107	0.2404	0.3915	0.5661	0.7673
hypercube (C_6)	64	Y	6	0.1255	0.2630	0.4150	0.5850	0.7776	
d	lower bound				0.0173	0.0718	0.1716	0.3333	0.5888
	simplex (S_d)	$d+1$	Y	d	0.0173	0.0718	0.1716	0.3333	0.5888
	orthoplex (O_d)	$2d$	Y	$2(d-1)$	0.0173	0.0718	0.1716	0.3333	0.5888
	expanded simplex (A_d)	$d(d+1)$	Y	$2(d-1)$	0.0173	0.0718	0.1716	0.3333	0.5888
	rectified orthoplex (D_d)	$2d(d-1)$	Y	$4(d-2)$	0.0173	0.0718	0.1716	0.3333	0.5888
	hypercube (C_d ; A orthogonal)	2^d	Y	d	0.0799	0.1800	0.3151	0.5201	0.7686
hypercube (C_d ; A Gaussian)	2^d	Y	d	0.1255	0.2630	0.4150	0.5850	0.7776	

Table 1. Parameters ρ for various spherical codes. Column “I?” denotes isogonal, and “ $|\mathcal{R}|$ ” the number of relevant vectors per code word. Sphere packings are from [Slo]. Rows labeled “spherical caps” are conjectured lower bounds (Conjecture 22). Superscripts refer to the number of caps minimizing ρ . Bold values indicate the best values ρ encountered up to this dimension. Results for $k = 1, 2, d$, were obtained analytically; for $k = 3, 4, 5, 6$ most results were obtained through numerical integration and Monte Carlo simulation. For large d and small θ , the numerical integration generally becomes less precise, and e.g. the fourth decimals may be off by one.

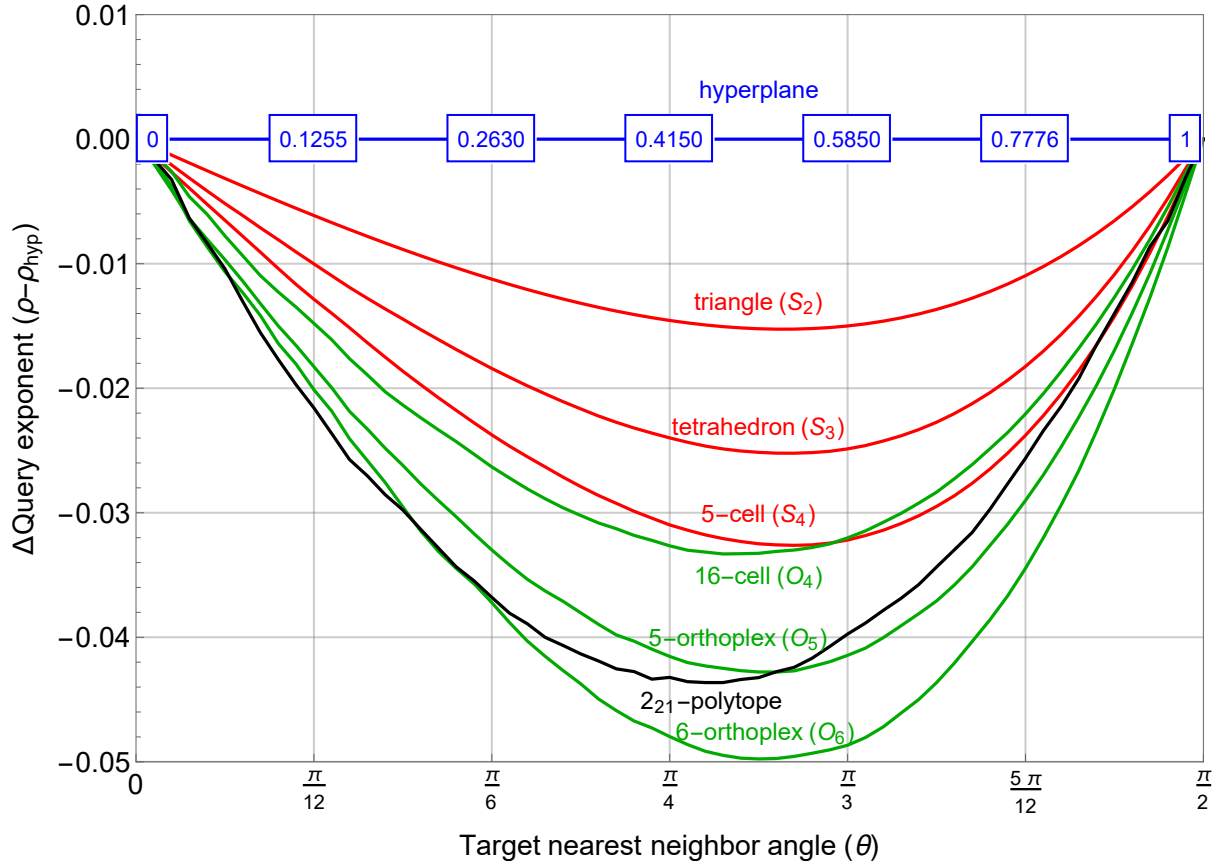


Fig. 1. Comparison of the improvements in the query exponent ρ over the hyperplane hashing approach of Charikar [Cha02] with query exponent ρ_{hyp} . The horizontal blue line denotes the baseline hyperplane hashing approach, with $\rho - \rho_{\text{hyp}} \equiv 0$. Lower curves denote improvements to ρ using various spherical codes. The measurements at the five vertical gridlines correspond to the values in Table 1. For instance, at $\theta = \pi/6$ the triangle has query exponent approximately 0.011 lower than hyperplane hashing (which has exponent 0.2630), leading to the estimate $\rho \approx 0.2520$; from Table 1 we get the more precise estimate $\rho \approx 0.2518$; while the theory in Section 5 allows us to compute ρ exactly through a closed-form expression. The polytopes in this figure are those achieving the lowest exponents ρ in their respective dimensions at one of these grid lines, as highlighted in boldface in Table 1.

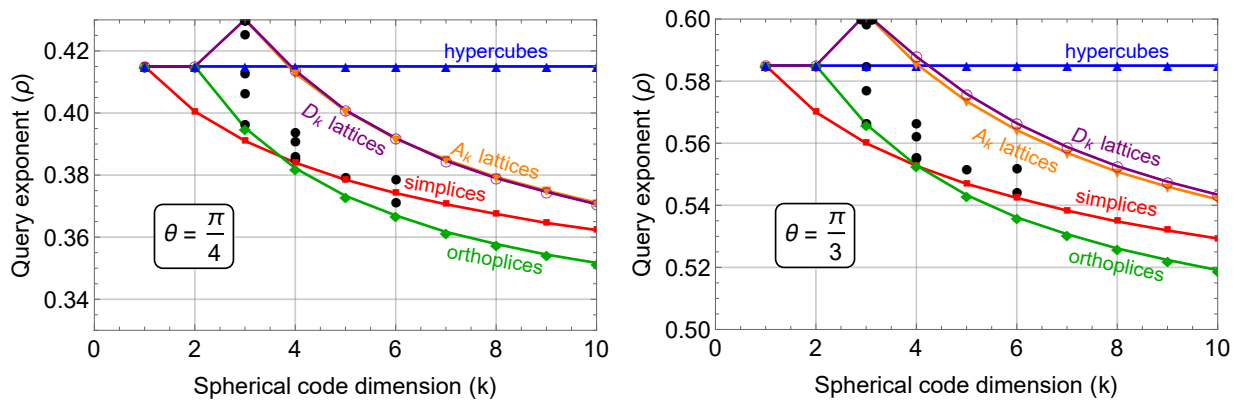


Fig. 2. Query exponents ρ for project-and-partition hash families based on the spherical codes listed in Table 1. Lower query exponents ρ are generally better, and for these hash families the best exponents ρ are achieved by the simplex for $k \leq 3$ and by the orthoplex for $k \geq 5$. For $k = 4$ the simplex and orthoplex are close, and which of the two achieves a better performance depends on the target nearest neighbor angle θ .

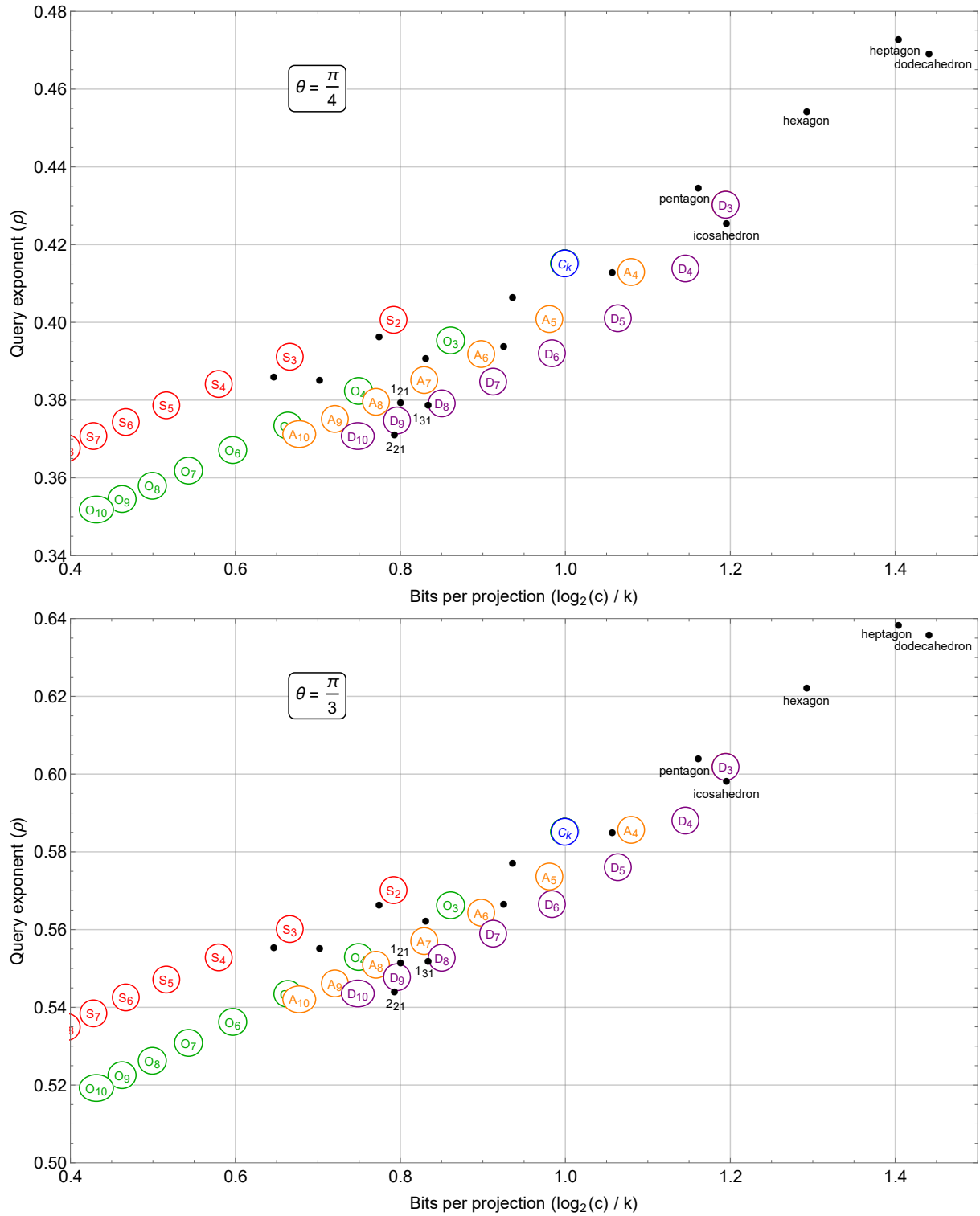


Fig. 3. A comparison between different spherical codes in terms of the query exponent ρ (vertical axis) and the bits of “information” extracted from each row of the projection matrix \mathbf{A} (horizontal axis). Codes further down generate hash functions with a more discriminative power, and codes further to the right require fewer random projections to compute hash values; further down and to the right is better. Hypercubes C_k all achieve the same ρ and $\log_2(c)/k$.

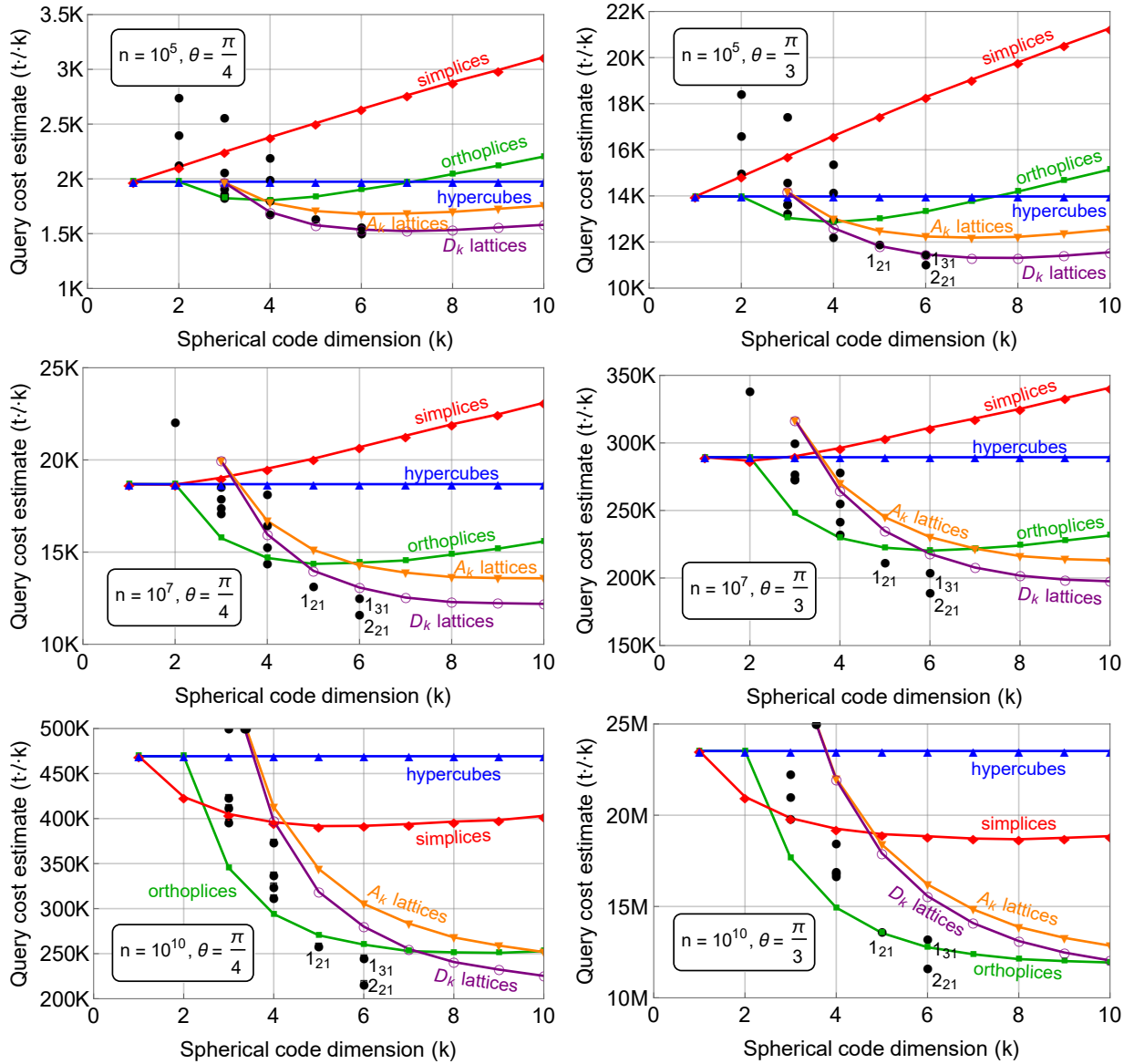


Fig. 4. Comparison of the query cost estimates $t \cdot \ell \cdot k$ for different parameters $n \in \{10^5, 10^7, 10^{10}\}$ and $\theta \in \{\frac{\pi}{4}, \frac{\pi}{3}\}$, when using $t = n^\rho$ hash tables and a hash length $\ell = \log(n)/\log(1/p_2)$. The curves correspond to the regular convex polytope families and the root lattice families A_k and D_k , while single black points for $k \leq 6$ correspond to spherical codes described in Table 1. As n increases, the role of a smaller ρ becomes bigger, and so larger spherical codes with smaller values ρ become more suitable choices. The cost of the projections increases linearly with k , while ρ decreases slowly with k , suggesting that for each n and θ there is an optimal spherical code dimension $k \ll d$ to project down to, and an optimal spherical code in this dimension to use. Note that other spherical codes than those from the five families of codes sometimes achieve better query cost estimates; in particular, the 2_{21} -polytope (which is connected to the E_6 lattice) may be useful in practice.

2 Preliminaries

Basic notation. Throughout the paper, we denote vectors in lower-case boldface (e.g. \mathbf{x}), and matrices in upright, upper-case boldface (e.g. \mathbf{A}). Coordinates of vectors and matrices are written without boldface (e.g. x_i and $A_{i,j}$). We write $\mathbf{x} \geq \mathbf{y}$ to denote the event that $x_i \geq y_i$ for all i . We write \mathbf{e}_i for the i th unit vector with a 1 on position i , and a 0 in all other coordinates. We write \mathbf{I}_k for the $k \times k$ identity matrix, and \mathbf{J}_k for the $k \times k$ matrix with all entries equal to 1. We write $\mathbf{K} = \mathbf{A} \otimes \mathbf{B}$ for the standard Kronecker (tensor) product of matrices; if $\mathbf{A} \in \mathbb{R}^{r_a \times c_a}$ and $\mathbf{B} \in \mathbb{R}^{r_b \times c_b}$, then $\mathbf{K} \in \mathbb{R}^{(r_a r_b) \times (c_a c_b)}$ is a matrix with entries $A_{i,j} B_{k,l}$. We write $\|\mathbf{x}\| = (\sum_i x_i^2)^{1/2}$ for the Euclidean norm of \mathbf{x} , and we denote the standard dot product in \mathbb{R}^k by $\langle \mathbf{x}, \mathbf{y} \rangle = \sum_i x_i y_i$. Given two vectors $\mathbf{x}, \mathbf{y} \in \mathbb{R}^k$, we further denote their mutual angle by

$$\phi(\mathbf{x}, \mathbf{y}) = \arccos \left\langle \frac{\mathbf{x}}{\|\mathbf{x}\|}, \frac{\mathbf{y}}{\|\mathbf{y}\|} \right\rangle. \quad (3)$$

Angles between vectors are invariant under scalar multiplication of either vector (i.e. $\phi(\lambda \mathbf{x}, \mu \mathbf{y}) = \phi(\mathbf{x}, \mathbf{y})$ for all $\lambda, \mu > 0$), and if \mathbf{A} is a rotation matrix (\mathbf{A} is orthogonal), then $\phi(\mathbf{A}\mathbf{x}, \mathbf{A}\mathbf{y}) = \phi(\mathbf{x}, \mathbf{y})$.

Geometry on the sphere. We write $\mathcal{S}^{k-1} = \{\mathbf{x} \in \mathbb{R}^k : \|\mathbf{x}\| = 1\}$ for the Euclidean unit sphere in k dimensions. We write μ for the standard Haar measure, so that the relative volume of $\mathcal{A} \subseteq \mathcal{S}^{k-1}$ on the sphere can be expressed as $\mu(\mathcal{A})/\mu(\mathcal{S}^{k-1})$. Let $\mathcal{C}_\alpha = \{\mathbf{x} \in \mathcal{S}^{k-1} : x_1 > \alpha\}$ denote a *spherical cap* of height $1 - \alpha$. Writing $I_x(a, b)$ for the regularized incomplete beta function, we can compute the volume of \mathcal{C}_α as [LK14]:

$$\frac{\mu(\mathcal{C}_\alpha)}{\mu(\mathcal{S}^{k-1})} = \frac{1}{2} I_{1-\alpha^2} \left(\frac{k-1}{2}, \frac{1}{2} \right). \quad (4)$$

Asymptotically (for large k), the above ratio scales as $k^{\Theta(1)} \cdot (1 - \alpha^2)^{k/2}$ [Sha59, BDGL16, ALRW17].

Spherical codes and Voronoi cells. Given a finite set of points (code words) $\mathcal{C} = \{\mathbf{c}_1, \dots, \mathbf{c}_c\} \subset \mathbb{R}^k$, the *Voronoi cells* of \mathcal{C} are subsets of \mathbb{R}^k , associating to each point $\mathbf{c}_i \in \mathcal{C}$ a Voronoi region

$$\mathcal{V}_i = \mathcal{V}_i(\mathcal{C}) = \{\mathbf{x} \in \mathbb{R}^k : \|\mathbf{x} - \mathbf{c}_i\| \leq \|\mathbf{x} - \mathbf{c}_j\|, \forall j = 1, \dots, c\}. \quad (5)$$

Note that $\bigcup_i \mathcal{V}_i = \mathbb{R}^k$, while $\sum_{i \neq j} \mu(\mathcal{V}_i \cap \mathcal{V}_j) / \mu(\mathcal{S}^{k-1}) = 0$; except for the boundaries between cells, which together have measure 0, this forms a proper partition of \mathbb{R}^k . For a partition of a space into Voronoi cells induced by \mathcal{C} , we write \mathcal{R}_i for the set of *relevant vectors* of $\mathbf{c}_i \in \mathcal{C}$, i.e. the vectors $\mathbf{c}_j \in \mathcal{C}$ such that $\mathcal{V}_i, \mathcal{V}_j$ share a non-trivial boundary. If $\mathcal{C} \subset \mathcal{S}^{k-1}$, we call \mathcal{C} a *spherical code*, and in that case the Voronoi cells take conical shapes, and are invariant under (positive) scalar multiplication; $\mathbf{x} \in \mathcal{V}_i$ iff $\mathbf{x}/\|\mathbf{x}\| \in \mathcal{V}_i$. Each pair of cells $\mathcal{V}_i, \mathcal{V}_j$ then shares a common point $\mathbf{0}$; for \mathbf{c}_j to be considered a relevant vector of \mathbf{c}_i , the intersection between $\mathcal{V}_i, \mathcal{V}_j$ must contain more than only $\mathbf{0}$. We further say a spherical code \mathcal{C} is *uniform* if the associated Voronoi partition satisfies $\mu(\mathcal{V}_i) = \mu(\mathcal{V}_j)$ for all i, j , and we say \mathcal{C} is *isogonal* (vertex-transitive) if, for each $\mathbf{c}_i, \mathbf{c}_j \in \mathcal{C}$, there exists an isometry f with $f(\mathbf{c}_i) = \mathbf{c}_j$ and $f(\mathcal{C}) = \mathcal{C}$.

Lattices and root systems. Given a set $\mathbf{B} = \{\mathbf{b}_1, \dots, \mathbf{b}_k\}$ of linearly independent vectors, we define the lattice $\mathcal{L} = \mathcal{L}(\mathbf{B}) = \{\sum_{i=1}^k \lambda_i \mathbf{b}_i : \lambda \in \mathbb{Z}^k\}$. A lattice \mathcal{L} is an *integral lattice* if for all $\mathbf{v}, \mathbf{w} \in \mathcal{L}$ we have $\langle \mathbf{v}, \mathbf{w} \rangle \in \mathbb{Z}$. A lattice \mathcal{L} is a *root lattice* if it is integral and generated by a set of roots $\mathbf{a} \in \mathcal{L}$ satisfying $\|\mathbf{a}\|^2 = 2$. Besides the three exceptional lattices E_6, E_7 and E_8 , the only irreducible root lattices are those from the following two families [Bro02]:

- A_k : Described as a subset of \mathbb{R}^{k+1} , this lattice has $k(k+1)$ roots $\mathbf{e}_i - \mathbf{e}_j$ for $i \neq j$.³
- D_k : This lattice has roots $\pm \mathbf{e}_i \pm \mathbf{e}_j$, for $i \neq j$. There are $2k(k-1)$ such roots.

Note that the roots of the root systems B_k and C_k are of different norms, and these sets of roots therefore do not define proper spherical codes.

Regular polytopes. Throughout the paper we will study spherical codes generated by *regular polytopes*, i.e. polytopes with regular facets and regular vertex figures. Besides several regular polytopes in low dimensions, there are only three families of regular polytopes in high dimensions.

- S_k : Described as a subset of \mathbb{R}^{k+1} , the k -simplex has vertices \mathbf{e}_i for $i = 1, \dots, k+1$.¹
- O_k : The k -orthoplex or k -cross polytope has $2k$ vertices of the form $\pm \mathbf{e}_i$, for $i = 1, \dots, k$.
- C_k : The hypercube in dimension k has 2^k vertices $\pm \mathbf{e}_1 \pm \dots \pm \mathbf{e}_k$, taking all possible signs.

Besides these infinite families, there are several regular polytopes in dimension up to four, such as the Platonic and Archimedean solids.

Probabilities. Given a set \mathcal{A} , we write $a \sim \mathcal{A}$ to denote the process of drawing a uniformly at random from \mathcal{A} . With slight abuse of notation, we similarly write $a \sim \xi$ to denote that a is drawn from a probability distribution ξ ; from the context it will be clear which case we are referring to. We write $\mathcal{N}(\mu, \sigma^2)$ for the (univariate) normal distribution with mean μ and variance σ^2 , and we write $\mathcal{N}(\boldsymbol{\mu}, \boldsymbol{\Sigma})$ for the multivariate normal distribution with mean $\boldsymbol{\mu}$ and correlation matrix $\boldsymbol{\Sigma}$. We refer to $\mathcal{N}(0, 1)$ and $\mathcal{N}(\mathbf{0}, \mathbf{I}_k)$ as the univariate and multivariate standard normal distributions.

3 A framework for nearest neighbor searching with spherical codes

In this section we will describe a framework for solving a natural average-case version of the nearest neighbor problem with well-chosen spherical codes, and we will show how the performance of these codes can be estimated and compared, to find the best spherical codes. In subsequent sections we will then apply this framework to different spherical codes.

3.1 The nearest neighbor problem

Let us start with a broad definition of the nearest neighbor problem, the topic of this paper.

Definition 3 (Nearest neighbor problem) *Given a data set $\mathcal{D} = \{\mathbf{p}_1, \dots, \mathbf{p}_n\} \subset \mathbb{R}^d$, the nearest neighbor problem asks to index \mathcal{D} in a data structure such that, when later given a query vector $\mathbf{q} \in \mathbb{R}^d$, one can quickly find a nearest neighbor $\mathbf{p}^* \in \mathcal{D}$ to \mathbf{q} .*

Depending on the similarity measure, which defines when points are considered nearby, and depending on how the above problem is modeled, different solutions exist. In this paper we will be concerned with the nearest neighbor problem for the angular distance, where the similarity between two vectors is measured by their angle:

$$\text{dist}(\mathbf{x}, \mathbf{y}) = \phi(\mathbf{x}, \mathbf{y}) = \arccos \left\langle \frac{\mathbf{x}}{\|\mathbf{x}\|}, \frac{\mathbf{y}}{\|\mathbf{y}\|} \right\rangle. \quad (6)$$

With this notion of similarity, two vectors are considered nearby if they have a small angle, and so for the nearest neighbor problem we are looking for the point $\mathbf{p}^* \in \mathcal{D}$ which has the smallest

³ As all vertices lie on a hyperplane, the vertices can be projected onto \mathbb{R}^k while preserving all mutual distances.

angle with the query vector \mathbf{q} . As the angle between two vectors is independent of their norms, this can equivalently be viewed as the nearest neighbor problem for the Euclidean distance on the unit sphere ($\mathcal{D} \subset \mathcal{S}^{d-1}$) by scaling all vectors to have norm 1: a small angle then corresponds to a small distance on the unit sphere through the following one-to-one relation between Euclidean distances and angles:

$$\mathbf{x}, \mathbf{y} \in \mathcal{S}^{d-1} \quad \implies \quad \frac{1}{2} \|\mathbf{x} - \mathbf{y}\|^2 = 1 - \cos \phi(\mathbf{x}, \mathbf{y}). \quad (7)$$

As described in e.g. [AR15, AIL⁺15, AR16, ALRW17], the angular nearest neighbor problem (or the Euclidean nearest neighbor problem on the unit sphere) is in a sense the canonical hard problem; through various reductions, a solution to the nearest neighbor problem for this problem would immediately yield an (efficient) algorithm for the nearest neighbor problem in the ℓ_1 and ℓ_2 -norms in all of \mathbb{R}^d . Studying this problem therefore may also be of interest when considering the nearest neighbor problem for other metrics.

Since it has long been known that solving this problem exactly for worst-case instances cannot be done in sublinear time in the size of the data set $n = |\mathcal{D}|$ [IM98, AR16], a large body of work has focused on *approximation* versions of this problem under *worst-case* assumptions, where an approximate solution $\hat{\mathbf{p}} \in \mathcal{D}$ with $\text{dist}(\hat{\mathbf{p}}, \mathbf{q}) \leq c \cdot \text{dist}(\mathbf{p}^*, \mathbf{q})$ suffices for solving the problem, given some approximation factor $c > 1$ and the exact nearest neighbor $\mathbf{p}^* \in \mathcal{D}$ to \mathbf{q} in \mathcal{D} . Here instead we will focus on methods for solving this problem *exactly* in sublinear time for *average-case* instances, by making suitable, natural assumptions on the distribution of the data points \mathbf{p}_i and the query vector \mathbf{q} .

Definition 4 (Nearest neighbor problem on the sphere) *Given a data set \mathcal{D} of size n drawn uniformly at random from \mathcal{S}^{d-1} , and a parameter $\theta \in (0, \frac{\pi}{2})$, the nearest neighbor problem on the sphere asks to index \mathcal{D} in a data structure such that, when later given a uniformly random query $\mathbf{q} \in \mathcal{S}^{d-1}$, we can quickly find a neighbor $\mathbf{p}^* \in \mathcal{D}$ with $\phi(\mathbf{p}^*, \mathbf{q}) \leq \theta$, or conclude that with high probability no such vector $\mathbf{p}^* \in \mathcal{D}$ exists.*

This description covers many applications where the data set and the query are indeed (close to) uniformly random, and we wish to detect highly similar objects in the database, if they exist. Note that there is often a one-to-one correspondence between such average-case, exact solutions and worst-case, approximate solutions – we can often substitute \mathcal{D} with a (worst-case) data set \mathcal{D}' with the guarantee that no vectors in $\mathcal{D}' \setminus \{\mathbf{p}^*\}$ have angle smaller than $\theta' > \theta$ with the query vector, and use the same algorithms in both cases.

3.2 Locality-sensitive hashing

To solve the nearest neighbor problem on the unit sphere, we will follow the celebrated *locality-sensitive hashing* framework, first introduced in [IM98]. Let us first restate the folklore definition of locality-sensitive hash function, slightly adjusted to fit our model of exact nearest neighbor searching for the angular distance for random data points.

Definition 5 (Locality-sensitive hash functions) *Let $c \in \mathbb{N}$. A set \mathcal{H} of hash functions $h : \mathbb{R}^d \rightarrow \{1, \dots, c\}$ is called (θ, p_1, p_2) -sensitive if (1) two vectors at an angle at most θ collide with probability at least p_1 ; and (2) two random vectors collide with probability at most p_2 :*

$$\Pr_{\substack{h \sim \mathcal{H} \\ \mathbf{x}, \mathbf{y} \sim \mathcal{S}^{d-1}}} (h(\mathbf{x}) = h(\mathbf{y}) \mid \phi(\mathbf{x}, \mathbf{y}) \leq \theta) \geq p_1, \quad \Pr_{\substack{h \sim \mathcal{H} \\ \mathbf{x}, \mathbf{y} \sim \mathcal{S}^{d-1}}} (h(\mathbf{x}) = h(\mathbf{y})) \leq p_2. \quad (8)$$

With slight abuse of notation, we will sometimes use p_1 and p_2 to refer to the actual probabilities above (rather than their lower and upper bounds, respectively). Now, assuming such hash functions exist, and they are efficiently evaluable⁴, we can build efficient nearest neighbor data structures as follows. After selecting suitable parameters ℓ and t , we construct t hash tables T_1, \dots, T_t , each consisting of c^ℓ hash buckets, corresponding to the concatenated outputs of ℓ randomly chosen hash functions $h_1, \dots, h_\ell \sim \mathcal{H}$ from our hash family. For each vector $\mathbf{p} \in \mathcal{D}$ and each hash table T_i , we compute its combined hash value, and insert \mathbf{p} in the corresponding hash bucket with label $(h_{i,1}(\mathbf{p}), \dots, h_{i,\ell}(\mathbf{p}))$. Then, given a query \mathbf{q} , for each hash table T_i we compute its corresponding hash bucket $(h_{i,1}(\mathbf{q}), \dots, h_{i,\ell}(\mathbf{q}))$, look up vectors stored in this hash bucket, and check if any of them have angle less than θ with \mathbf{q} . After going through all the hash tables, we hope to have encountered the nearest neighbor $\mathbf{p}^* \in \mathcal{D}$ in one of these hash tables, while hopefully the total amount of work done at this point (computing hashes, doing hash table look-ups, going through potential nearest neighbors in the hash buckets) is still sublinear in n .

Besides the initialization costs of locality-sensitive hashing (e.g. setting up the hash functions, and initializing and populating the hash tables), the query costs can be divided in two main costs: (1) computing $t \cdot \ell$ hash values and doing t lookups in memory to locate the right hash buckets; and (2) going through all potential nearest neighbors encountered in these hash buckets, to find a solution. By choosing ℓ and t carefully, as a function of n, θ, p_1, p_2 , we can balance these costs and minimize the query costs as stated in the folklore result below.

Proposition 6 (Locality-sensitive hashing for the nearest neighbor problem) *Let \mathcal{H} be an efficiently evaluable (θ, p_1, p_2) -sensitive hash family, and let*

$$\rho = \frac{\log 1/p_1}{\log 1/p_2}, \quad \ell = \frac{\log n}{\log 1/p_2}, \quad t = O(n^\rho). \quad (9)$$

Then, using locality-sensitive hashing with these parameters, we can solve the nearest neighbor problem with the following costs:

1. *Initializing and populating the data structure can be done in time $\tilde{O}(n^{1+\rho})$;*
2. *The data structure requires $\tilde{O}(n^{1+\rho})$ memory to store;*
3. *With prob. ≥ 0.99 , within time $\tilde{O}(n^\rho)$ the algorithm finds a neighbor at angle $\leq \theta$, if it exists.*

Here \tilde{O} hides multiplicative factors which are polynomial in d and $\log n$, while the success probability can be fine-tuned through the leading constant of t ; a larger t leads to a higher success probability.

Note that the memory and query costs scale as $n^{1+\rho}$ and n^ρ respectively, and so the goal is to find a locality-sensitive hash family \mathcal{H} minimizing the associated parameter ρ , for the parameter θ of interest, preferably with an efficient decoding algorithm. Beyond this point, we will mostly ignore all other aspects of locality-sensitive hashing, and focus on finding families \mathcal{H} minimizing ρ ; in Section 10 we will come back to these practical aspects of locality-sensitive hashing.

3.3 Space partitions

Various locality-sensitive hash families achieving sublinear query times have been proposed over time. Although some are strictly more efficient than others, often there is a trade-off between e.g. the different performances for different angles θ (approximation factors c); the asymptotic efficiency for large d and n ; and the practical performance for small/moderate values d and n . Examples of hash families for the angular distance from the literature include:

⁴ Being able to compute $h(\mathbf{x})$ given \mathbf{x} in $n^{o(1)}$ time may be sufficient to guarantee the stated asymptotic time complexities, but in practice a superpolynomial decoding cost $d^{\omega(1)}$ may already render the method impractical.

- The fast and practical hyperplane-based approach of Charikar [Cha02];
- The asymptotically optimal cross-polytope hash family [TT07, ER08, TT09, AIL⁺15, KW17];
- The closely related (asymptotically optimal) simplex hash family [TT07, TT09];
- The hypercube hash family [TT07, TT09, Laa17];
- Hash families based on spherical caps [AI06, AINR14, BDGL16, ALRW17];
- Approaches based on using suitable integer lattices [AI06, CDGG18].

More recently, it has been shown that deviating from the locality-sensitive hashing framework (by relaxing the condition that h induces a proper partition of the space) may lead to better asymptotic results in certain applications [BL16, BDGL16, ALRW17, Chr17]. However, for data sets of subexponential size ($n = 2^{o(d)}$), the best locality-sensitive hash methods achieve the same asymptotic performance as these locality-sensitive filters, and appear to perform better in practice [AIL⁺15, RS16, Ber16, ABF17b, ABF17a]. Here we restrict our attention to locality-sensitive hash families generated by proper partitions of the unit sphere.

Out of the above methods, the hyperplane-based approach of Charikar [Cha02] is often (one of) the most efficient in practice, due to its simple decoding algorithm which can be made extremely fast with heuristic tweaks [Ach01]. For sufficiently large d and n , the cross-polytope hash family will perform better, but e.g. in applications in cryptography, the cross-over point between hyperplane hashing and “optimal” hash families was found to be quite high [Laa15, BL16, BDGL16, MLB17]. Rather than only focusing on asymptotic performance, we will search for hash families with similar properties to the hyperplane-based approach, ideally allowing us to interpolate between the fast hyperplane LSH and the asymptotically superior cross-polytope LSH.

3.4 Project-and-partition

A common approach for locality-sensitive hashing encompasses two steps:

Project. Given vectors $\mathbf{x} \in \mathbb{R}^d$, we first project down onto a k -dimensional subspace through a random projection matrix $\mathbf{A} \in \mathbb{R}^{k \times d}$, to obtain $\mathbf{A}\mathbf{x} \in \mathbb{R}^k$. This projection is not lossless, and mutual distances/angles generally cannot be perfectly preserved through this transformation, but ideally these distances are preserved as best as possible. For this, here we generate \mathbf{A} by choosing each entry independently as a standard normal random variable. Note that with high probability, for constant $k = O(1)$ and large d the k rows of \mathbf{A} will be approximately orthogonal and have approximately the same norms [Jia06]. Through the above definition of \mathbf{A} however, we eliminate the dependence on d in the analysis of the collision probabilities p_1 and p_2 – the distribution of any particular column of \mathbf{A} is independent of d .

Partition. Using a partition of \mathbb{R}^k into c regions, we assign a hash value to \mathbf{x} according to the region $\mathbf{A}\mathbf{x}$ landed in, using a decoding function $\text{dec} : \mathbb{R}^k \rightarrow \{1, \dots, c\}$. A natural choice for the partition is to use the Voronoi cells induced by a suitable code $\mathcal{C} \subset \mathbb{R}^k$ of size $|\mathcal{C}| = c$. When all code words $\mathbf{c} \in \mathcal{C}$ have the same (unit) length, \mathcal{C} forms a spherical code, and in the remainder we will exclusively focus on such codes $\mathcal{C} \subset \mathcal{S}^{k-1}$.

Given a spherical code \mathcal{C} , we thus obtain the following hash function family \mathcal{H} .

Definition 7 (Spherical code hash families) *Let $\mathcal{C} \subset \mathcal{S}^{k-1}$ be a spherical code of size $|\mathcal{C}| = c$, and let $\text{dec} : \mathbb{R}^k \rightarrow \{1, \dots, c\}$ be a decoding algorithm for the Voronoi cells of \mathcal{C} . Then we associate to \mathcal{C} hash functions $h = h_{\mathbf{A}}$ as follows:*

$$h_{\mathbf{A}}(\mathbf{x}) = \text{dec}(\mathbf{A}\mathbf{x}). \tag{10}$$

For the corresponding hash family \mathcal{H} , sampling $h \sim \mathcal{H}$ corresponds to sampling $\mathbf{A} \sim \mathcal{N}(0, 1)^{k \times d}$.

Observe that in all cases the decoding step can be done in time $O(ck)$, by computing all distances between $\mathbf{A}\mathbf{x}$ and code words $\mathbf{c} \in \mathcal{C}$, but for some codes with additional structure, faster decoding algorithms may exist. Projections can naively be computed in time $O(dk)$, for a total hash time complexity of $O(dk + ck)$.

As an example, for hyperplane LSH [Cha02] we have $k = 1$ (i.e. we project onto a line), and the matrix $\mathbf{A} \in \mathbb{R}^{1 \times d}$ is a vector drawn from a spherically-symmetric distribution (e.g. a Gaussian distribution). The partition is then defined by the Voronoi cells of the one-dimensional spherical code $\mathcal{C} = \{-1, 1\}$; the sign of the inner product $\mathbf{A}\mathbf{x} \in \mathbb{R}$ determines whether the hash value equals 0 or 1.

3.5 Orthant probabilities

Without loss of generality, let $\mathbf{x} = (1, 0, \dots, 0)$ and, in case of a predetermined angle θ with \mathbf{x} , let $\mathbf{y} = (\cos \theta, \sin \theta, 0, \dots, 0)$. Denoting the k -dimensional columns of \mathbf{A} by \mathbf{a}_i , observe that $\mathbf{A}\mathbf{x} = \mathbf{a}_1$ and $\mathbf{A}\mathbf{y} = (\cos \theta)\mathbf{a}_1 + (\sin \theta)\mathbf{a}_2$. Note that while \mathbf{x} and \mathbf{y} have angle *exactly* θ , $\mathbf{A}\mathbf{x}$ and $\mathbf{A}\mathbf{y}$ only have angle *approximately* θ , depending on how orthogonal the two random vectors $\mathbf{a}_1, \mathbf{a}_2 \sim \mathcal{N}(0, 1)^k$ are. This means that we can compute p_1 as follows:

$$p_1 = \Pr_{\substack{h \sim \mathcal{H} \\ \mathbf{x}, \mathbf{y} \sim \mathcal{S}^{d-1}}} (h(\mathbf{x}) = h(\mathbf{y}) \mid \phi(\mathbf{x}, \mathbf{y}) = \theta) \quad (11)$$

$$= \sum_{i=1}^c \Pr_{\mathbf{a}_1, \mathbf{a}_2 \sim \mathcal{N}(\mathbf{0}, \mathbf{I}_k)} (\text{dec}(\mathbf{a}_1) = \text{dec}(\mathbf{a}_1 \cos \theta + \mathbf{a}_2 \sin \theta) = \mathbf{c}_i). \quad (12)$$

For two independently sampled vectors $\mathbf{x}, \mathbf{y} \sim \mathcal{S}^{d-1}$, also $\mathbf{A}\mathbf{x}$ and $\mathbf{A}\mathbf{y}$ are independent. Given any spherical code $\mathcal{C} = \{\mathbf{c}_1, \dots, \mathbf{c}_c\} \in \mathcal{S}^{k-1}$, we can thus describe the probability p_2 as follows:

$$p_2 = \Pr_{\substack{h \sim \mathcal{H} \\ \mathbf{x}, \mathbf{y} \sim \mathcal{S}^{d-1}}} (h(\mathbf{x}) = h(\mathbf{y})) \quad (13)$$

$$= \sum_{i=1}^c \Pr_{\mathbf{a}_1 \sim \mathcal{N}(\mathbf{0}, \mathbf{I}_k)} (\text{dec}(\mathbf{a}_1) = \mathbf{c}_i)^2 \quad (14)$$

$$= \frac{1}{\mu(\mathcal{S}^{d-1})^2} \sum_{i=1}^c \mu(\mathcal{V}_i)^2. \quad (15)$$

Here $\mathcal{V}_i \subset \mathbb{R}^k$ denotes the Voronoi region associated to \mathbf{c}_i , and $\mu(\mathcal{V}_i)$ its measure. Note that for a size- c partition of \mathbb{R}^k , p_2 is smallest if all regions have the same size, in which case $p_2 = 1/c$.

To further study p_1 , for general codes \mathcal{C} by definition we have $\text{dec}(\mathbf{x}) = \mathbf{c}_i$ if and only if $\|\mathbf{x} - \mathbf{c}_i\| \leq \|\mathbf{x} - \mathbf{c}_j\|$ for all $j = 1, \dots, c$.⁵ Since we assume that \mathcal{C} is a spherical code, this is equivalent to $\langle \mathbf{x}, \mathbf{c}_i \rangle \geq \langle \mathbf{x}, \mathbf{c}_j \rangle$ for all $j = 1, \dots, c$, or equivalently $\langle \mathbf{x}, \mathbf{c}_i - \mathbf{c}_j \rangle \geq 0$ for all $j = 1, \dots, c$. The event that $\mathbf{x} \in \mathbb{R}^k$ is mapped to the hash region corresponding to \mathbf{c}_i (i.e. $\mathbf{x} \in \mathcal{V}_i$) can thus equivalently be described by the following matrix inequality:

$$\begin{bmatrix} - & (\mathbf{c}_i - \mathbf{c}_1) & - \\ - & (\mathbf{c}_i - \mathbf{c}_2) & - \\ & \dots & \\ - & (\mathbf{c}_i - \mathbf{c}_c) & - \end{bmatrix} \cdot \begin{bmatrix} | \\ | \\ | \\ | \end{bmatrix} \geq \begin{bmatrix} | \\ | \\ | \\ | \end{bmatrix}. \quad (16)$$

⁵ For simplicity we ignore cases where \mathbf{x} lies on the boundary between two Voronoi cells and decoding is not unique, as the boundaries together have measure 0.

Let \mathbf{C}_i denote the matrix on the left hand side above, with rows $\mathbf{c}_i - \mathbf{c}_j$ for $j = 1, \dots, c$. Recall that for the event of two θ -correlated random vectors to both be mapped to \mathbf{c}_i , we need $\mathbf{C}_i \mathbf{x} \geq \mathbf{0}$ to hold for both $\mathbf{x} = \mathbf{a}_1$ and $\mathbf{x} = (\cos \theta) \mathbf{a}_1 + (\sin \theta) \mathbf{a}_2$, where $\mathbf{a}_1, \mathbf{a}_2 \sim \mathcal{N}(\mathbf{0}, \mathbf{I}_k)$. The probability p_1 can thus be described by a $2k$ -dimensional system of inequalities:

$$p_1 = \sum_{i=1}^c \Pr_{\mathbf{a}_1, \mathbf{a}_2 \sim \mathcal{N}(\mathbf{0}, \mathbf{I}_k)} \left(\left[\begin{array}{c|c} \mathbf{C}_i & \mathbf{0} \\ \hline (\cos \theta) \mathbf{C}_i & (\sin \theta) \mathbf{C}_i \end{array} \right] \begin{bmatrix} \mathbf{a}_1 \\ \mathbf{a}_2 \end{bmatrix} \geq \begin{bmatrix} \mathbf{0} \\ \mathbf{0} \end{bmatrix} \right) \quad (17)$$

$$= \sum_{i=1}^c \Pr_{\mathbf{z} \sim \mathcal{N}(\mathbf{0}, \mathbf{I}_{2k})} \left(\left\{ \begin{bmatrix} 1 & 0 \\ \cos \theta & \sin \theta \end{bmatrix} \otimes \mathbf{C}_i \right\} \mathbf{z} \geq \mathbf{0} \right). \quad (18)$$

Here \otimes denotes the standard Kronecker product for matrices. Note that if $\mathbf{z} \sim \mathcal{N}(\mathbf{0}, \mathbf{I}_{2k})$, then $\mathbf{z}' = \mathbf{B} \mathbf{z} \sim \mathcal{N}(\mathbf{0}, \mathbf{B} \mathbf{B}^T)$. Furthermore, using $(\mathbf{A} \otimes \mathbf{B}) \cdot (\mathbf{A} \otimes \mathbf{B})^T = (\mathbf{A} \mathbf{A}^T) \otimes (\mathbf{B} \mathbf{B}^T)$ for arbitrary \mathbf{A} and \mathbf{B} , we obtain:

$$p_1 = \sum_{i=1}^c \Pr_{\mathbf{z} \sim \mathcal{N}(\mathbf{0}, \mathbf{\Sigma}_i)} (\mathbf{z} \geq \mathbf{0}), \quad \mathbf{\Sigma}_i = \begin{bmatrix} 1 & \cos \theta \\ \cos \theta & 1 \end{bmatrix} \otimes (\mathbf{C}_i \mathbf{C}_i^T). \quad (19)$$

The probabilities above are also known as *orthant probabilities* for the multivariate normal distribution with covariance matrix $\mathbf{\Sigma}_i$. For completeness, note that p_2 can equivalently be described as an orthant probability, as:

$$p_2 = \sum_{i=1}^c \Pr_{\mathbf{z} \sim \mathcal{N}(\mathbf{0}, \mathbf{\Pi}_i)} (\mathbf{z} \geq \mathbf{0}), \quad \mathbf{\Pi}_i = \begin{bmatrix} 1 & 0 \\ 0 & 1 \end{bmatrix} \otimes \mathbf{C}_i \mathbf{C}_i^T, \quad (20)$$

$$= \sum_{i=1}^c \Pr_{\mathbf{z} \sim \mathcal{N}(\mathbf{0}, \mathbf{\Theta}_i)} (\mathbf{z} \geq \mathbf{0})^2, \quad \mathbf{\Theta}_i = \mathbf{C}_i \mathbf{C}_i^T, \quad (21)$$

This description is computationally more difficult to work with than the approach using volumes of the corresponding Voronoi cells, as in Equation (15). To summarize, the above derivation can be seen as a proof of the following theorem. Here $\text{dec}(\cdot) = \text{dec}_C(\cdot)$ denotes a decoding function for the corresponding spherical code, in terms of its Voronoi cells \mathcal{V}_i : $\text{dec}(\mathbf{x}) = i$ if $\mathbf{x} \in \mathcal{V}_i$ lies closer to \mathbf{c}_i than to all other code words $\mathbf{c}_j \in \mathcal{C}$.

Theorem 8 (Spherical code locality-sensitive hashing). *Let $\mathcal{C} = \{\mathbf{c}_1, \dots, \mathbf{c}_c\} \subset \mathcal{S}^{k-1}$ be a k -dimensional spherical code, and for $i = 1, \dots, c$, let $\mathbf{C}_i \in \mathbb{R}^{c \times k}$ denote the matrix whose j^{th} row is the vector $\mathbf{c}_i - \mathbf{c}_j$. Let \mathcal{H} consist of functions $h = h_{\mathbf{A}}$ of the form:*

$$h(\mathbf{x}) = \text{dec}(\mathbf{A} \mathbf{x}) \in \{1, \dots, c\}, \quad \mathbf{A} \sim \mathcal{N}(0, 1)^{k \times d}. \quad (22)$$

Then for any $\theta \in (0, \frac{\pi}{2})$, \mathcal{H} is a (θ, p_1, p_2) -sensitive hash family, with:

$$p_1 = \sum_{i=1}^c \Pr_{\mathbf{z} \sim \mathcal{N}(\mathbf{0}, \mathbf{\Sigma}_i)} (\mathbf{z} \geq \mathbf{0}), \quad \mathbf{\Sigma}_i = \begin{bmatrix} 1 & \cos \theta \\ \cos \theta & 1 \end{bmatrix} \otimes (\mathbf{C}_i \mathbf{C}_i^T), \quad p_2 = \frac{1}{\mu(\mathcal{S}^{d-1})^2} \sum_{i=1}^c \mu(\mathcal{V}_i)^2. \quad (23)$$

Note again that, by our choice of \mathbf{A} , the parameters p_1, p_2 are *independent* of d . For large $d \gg k$, choosing $\mathbf{A} \sim \mathcal{N}(0, 1)^{k \times d}$ or choosing \mathbf{A} to have orthogonal, unit-norm rows is essentially equivalent [DF87, Jia06]. For smaller $d \approx k$ however, these definitions are not the same, and it may be worthwhile to use orthogonal rows instead, to decrease the distortion of mutual distances by the projection \mathbf{A} . For instance, when using dense d -dimensional spherical codes for partitions, it may be impossible for two almost-orthogonal vectors to be in the same hash region, and p_2 may quickly approach 0 while p_1 remains large. Although our study may lead to advances and insights in the regime of $k \approx d$ as well, the main topic of interest here however is to first project down onto a k -dimensional space with $k \ll d$, and then use a suitable spherical code there for partitions.

3.6 Special spherical codes

For special classes of spherical codes, the expressions of Theorem 8 can be further simplified. We state two specific cases of interest below. First, if \mathcal{C} is such that the Voronoi cells of the vertices each cover an equal part of the sphere, i.e. $\mu(\mathcal{V}_i) = \mu(\mathcal{V}_j)$ for all i and j , then we get the following slightly simplified corollary. Note that given a fixed code size c , the value p_2 is minimized exactly when all Voronoi cells are of equal size. As we want to minimize $\rho = \rho(p_1, p_2)$ which is an increasing function of p_2 , this suggests that using such codes may well lead to the best results.⁶

Corollary 9 (Collision probabilities for uniform spherical codes) *Let $\mathcal{C} = \{\mathbf{c}_1, \dots, \mathbf{c}_c\} \subset S^{k-1}$ be a k -dimensional uniform spherical code, in the sense that $\mu(\mathcal{V}_i) = \mu(\mathcal{V}_j)$ for all i, j . Let \mathbf{C}_i and \mathcal{H} be as in Theorem 8. Then for any $\theta \in (0, \frac{\pi}{2})$, \mathcal{H} is a (θ, p_1, p_2) -sensitive hash family, with*

$$p_1 = \sum_{i=1}^c \Pr_{\mathbf{z} \sim \mathcal{N}(\mathbf{0}, \boldsymbol{\Sigma}_i)}(\mathbf{z} \geq \mathbf{0}), \quad \boldsymbol{\Sigma}_i = \begin{bmatrix} 1 & \cos \theta \\ \cos \theta & 1 \end{bmatrix} \otimes (\mathbf{C}_i \mathbf{C}_i^T), \quad p_2 = 1/c. \quad (24)$$

In case \mathcal{C} has many symmetries, and in particular is *isogonal* (vertex-transitive), then Theorem 8 can be further simplified, as in that case all hash regions are equivalent, and only one of the orthant probabilities needs to be evaluated to determine p_1, p_2 and ρ . Note that by definition, isogonal codes are a subset of the uniform spherical codes above.

Corollary 10 (Collision probabilities for isogonal spherical codes) *Let $\mathcal{C} = \{\mathbf{c}_1, \dots, \mathbf{c}_c\} \subset S^{k-1}$ be a k -dimensional isogonal spherical code, in the sense that for each $\mathbf{c}_i, \mathbf{c}_j \in \mathcal{C}$, there exists an isometry f with $f(\mathbf{c}_i) = \mathbf{c}_j$ and $f(\mathcal{C}) = \mathcal{C}$. Let \mathbf{C}_i and \mathcal{H} be as in Theorem 8. Then for any $\theta \in (0, \frac{\pi}{2})$, \mathcal{H} is a (θ, p_1, p_2) -sensitive hash family, with:*

$$p_1 = c \cdot \Pr_{\mathbf{z} \sim \mathcal{N}(\mathbf{0}, \boldsymbol{\Sigma}_1)}(\mathbf{z} \geq \mathbf{0}), \quad \boldsymbol{\Sigma}_1 = \begin{bmatrix} 1 & \cos \theta \\ \cos \theta & 1 \end{bmatrix} \otimes (\mathbf{C}_1 \mathbf{C}_1^T), \quad p_2 = 1/c. \quad (25)$$

For isogonal codes, computing the query exponent ρ comes down to computing a single orthant probability.

3.7 Relevant vectors

Finally, the computations of the collision probabilities p_1 and p_2 for a given spherical code can sometimes be simplified by reducing the number of conditions that define when a point is decoded to a given code word. Recall that the matrix \mathbf{C}_i , containing difference vectors $\mathbf{c}_i - \mathbf{c}_j$ as its rows, originates from the equivalence below:

$$\text{dec}(\mathbf{x}) = i \iff \forall \mathbf{c}_j \in \mathcal{C} : \|\mathbf{x} - \mathbf{c}_i\| \leq \|\mathbf{x} - \mathbf{c}_j\| \iff \forall \mathbf{c}_j \in \mathcal{C} : \langle \mathbf{x}, \mathbf{c}_i - \mathbf{c}_j \rangle \geq 0. \quad (26)$$

In many cases however, we can already conclude that $\text{dec}(\mathbf{x}) = i$ by only computing some of the distances $\|\mathbf{x} - \mathbf{c}_j\|$ – if \mathbf{x} is closer to \mathbf{c}_i than to any of the closest neighbors of \mathbf{c}_i in \mathcal{C} , then it must be closest to \mathbf{c}_i . More generally, we may define $\mathcal{R}_i \subseteq \mathcal{C}$ as the set of relevant vectors for \mathbf{c}_i , i.e. those vectors $\mathbf{c}_j \in \mathcal{C}$ whose Voronoi cells \mathcal{V}_j share a non-trivial boundary with \mathcal{V}_i . The conditions to verify that decoding \mathbf{x} results in i may then be simplified:

$$\text{dec}(\mathbf{x}) = i \iff \forall \mathbf{c}_j \in \mathcal{R}_i : \|\mathbf{x} - \mathbf{c}_i\| \leq \|\mathbf{x} - \mathbf{c}_j\| \iff \forall \mathbf{c}_j \in \mathcal{R}_i : \langle \mathbf{x}, \mathbf{c}_i - \mathbf{c}_j \rangle \geq 0. \quad (27)$$

⁶ The stated intuition does not provide a formal proof that ρ is minimized when all Voronoi cells have the same volume, as there is also an intricate dependence of p_1 (and ρ) on the shape of the Voronoi cells. If all Voronoi cells are of equal size, but their shapes are “bad”, then the resulting code may not be useful in our framework.

Computationally, for evaluating the orthant probabilities in p_1 in Theorem 8, this allows us to replace the matrix \mathbf{C}_i (with c rows $\mathbf{c}_i - \mathbf{c}_j$ for $\mathbf{c}_j \in \mathcal{C}$), with a smaller matrix $\hat{\mathbf{C}}_i$ (consisting of $|\mathcal{R}_i|$ rows $\mathbf{c}_i - \mathbf{c}_j$ for $\mathbf{c}_j \in \mathcal{R}_i$). This can significantly reduce the dimensionality of the resulting orthant probability problem, and this may assist in evaluating p_1 more accurately via numerical integration when no closed form expression is available.

Proposition 11 (Computing collision probabilities using relevant vectors) *Theorem 8 and Corollaries 9 and 10 remain valid when we replace the matrices $\mathbf{C}_i \in \mathbb{R}^{c \times k}$ by $\hat{\mathbf{C}}_i \in \mathbb{R}^{|\mathcal{R}_i| \times k}$, consisting of the rows $\mathbf{c}_i - \mathbf{c}_j$ with $\mathbf{c}_j \in \mathcal{R}_i$.*

With this general framework in hand, we can now compute collision probabilities for arbitrary spherical codes, and compute the resulting nearest neighbor exponents ρ , given \mathcal{C} and θ .

4 One-dimensional codes

Let us first illustrate the above framework by rederiving the hyperplane locality-sensitive hashing results of Charikar [Cha02]. For the 1-dimensional unit sphere $\mathcal{S}^0 = \{(-1), (1)\}$, there is only one choices for a spherical code $\mathcal{C} \subseteq \mathcal{S}^0$ of size at least two, namely $\mathcal{C} = \{(-1), (1)\}$. This code is an isogonal code, and $\mathcal{R}_{(1)} = \{(-1)\}$ and $\mathcal{R}_{(-1)} = \{(1)\}$ are the relevant vectors. As in Proposition 11, $\hat{\mathbf{C}}_1$ consists of one row, containing the vector $(1) - (-1) = (2)$. By Corollary 10 and Proposition 11, we can compute the collision probabilities, after projecting down using a random vector $\mathbf{A} \sim \mathcal{N}(0, 1)^{1 \times d}$, as:

$$p_1 = 2 \cdot \Pr_{\mathbf{z} \sim \mathcal{N}(\mathbf{0}, \Sigma_1)}(\mathbf{z} \geq \mathbf{0}), \quad \Sigma_1 = \begin{bmatrix} 1 & \cos \theta \\ \cos \theta & 1 \end{bmatrix} \otimes (4), \quad p_2 = 1/2. \quad (28)$$

For p_1 , observe that $\Pr_{\mathbf{z} \sim \mathcal{N}(\mathbf{0}, \Sigma_1)}(\mathbf{z} \geq \mathbf{0}) = \Pr_{\mathbf{z} \sim \mathcal{N}(\mathbf{0}, \mu \cdot \Sigma_1)}(\mathbf{z} \geq \mathbf{0})$ for all scalars μ . We can thus eliminate the factor 4, and we are left with a standard orthant probability for the bivariate normal distribution with covariance $\cos \theta$. The derivation of a closed-form formula for the orthant probability of the bivariate normal distribution is often attributed to Sheppard in the late 1800s [She99], who showed that the orthant probability for the bivariate normal distribution with Pearson correlation coefficient a is:

$$\Sigma = \begin{bmatrix} 1 & a \\ a & 1 \end{bmatrix} \implies \Pr_{(z_1, z_2) \sim \mathcal{N}(\mathbf{0}, \Sigma)}(z_1 \geq 0, z_2 \geq 0) = \frac{\pi - \arccos a}{2\pi}. \quad (29)$$

For our application, this implies the well-known result of Charikar [Cha02], stated below.

Proposition 12 (Collision probabilities for antipodal codes) *Let \mathcal{C} consist of two antipodal points on the unit sphere. Then the corresponding project-and-partition hash family \mathcal{H} is (θ, p_1, p_2) -sensitive, with:*

$$p_1 = 1 - \frac{\theta}{\pi}, \quad p_2 = \frac{1}{2}. \quad (30)$$

For the nearest neighbor query exponent $\rho = \log p_1 / \log p_2$, a simple computation leads to e.g. $\rho = \log_2(3/2) \approx 0.5850$ for $\theta = \frac{\pi}{3}$. Table 1 lists several query exponents ρ for this hash family, for different parameters $\theta \in \frac{\pi}{12}\{1, 2, 3, 4, 5\}$. Note that for $\theta \rightarrow 0$ we have $p_1 \rightarrow 1$ and $\rho \rightarrow 0$, while for $\theta \rightarrow \frac{\pi}{2}$ we have $p_1 \rightarrow p_2 = \frac{1}{2}$ and $\rho \rightarrow 1$, as expected.

5 Two-dimensional codes

The simplest previously unstudied case is to project down onto a two-dimensional subspace through a random projection matrix $\mathbf{A} \sim \mathcal{N}(0, 1)^{2 \times d}$, and to use a suitable spherical code on the two-dimensional sphere (circle) to divide these projected vectors into hash buckets. Using two (antipodal) points on the circle would be equivalent to using the one-dimensional hyperplane hashing described above, so the non-trivial cases start at spherical codes of size at least three.

5.1 Two-dimensional isogonal spherical codes

The following theorem summarizes the collision probabilities for what is arguably the most natural choice for a spherical code on the circle, which is to use any number of equidistributed points on the circle (i.e. to use the vertices of a regular polygon to partition the sphere).

Theorem 13 (Collision probabilities for regular polygons). *Let $\mathcal{C} \subset \mathcal{S}^1$ consist of the vertices of the regular c -gon, for $c \geq 2$, and let $\theta \in (0, \frac{\pi}{2})$. Then the corresponding project-and-partition hash family \mathcal{H} is (θ, p_1, p_2) -sensitive, with:*

$$p_1 = \frac{1}{c} + c \left(\frac{\pi - \theta}{2\pi} \right)^2 - c \left(\frac{\arccos(-\cos \theta \cos \frac{2\pi}{c})}{2\pi} \right)^2, \quad p_2 = 1/c. \quad (31)$$

To prove the above result, we will first derive the shape of the correlation matrix below.

Lemma 1 (The correlation matrix for regular polygons). *Let $\mathcal{C} \subset \mathcal{S}^1$ consist of the vertices of the regular c -gon, for $c \geq 2$. Then the correlation matrix Σ_1 in Theorem 10 (Prop. 11) satisfies:*

$$\Sigma_1 = 2(1 - \cos \frac{2\pi}{c}) \cdot \begin{bmatrix} 1 & \cos \theta \\ \cos \theta & 1 \end{bmatrix} \otimes \begin{bmatrix} 1 & -\cos \frac{2\pi}{c} \\ -\cos \frac{2\pi}{c} & 1 \end{bmatrix}. \quad (32)$$

Proof. Without loss of generality⁷, let us fix one vertex of \mathcal{C} at $(1, 0)$. For ease of notation, let us write $c_j = \cos \frac{2j\pi}{c}$ and $s_j = \sin \frac{2j\pi}{c}$, so that $\mathcal{C} = \{(c_j, s_j) : j = 1, \dots, c\}$. Now, a point in \mathbb{R}^2 is closest to $\mathbf{c}_c = (1, 0)$ out of all code words in \mathcal{C} iff it lies closer to $(1, 0)$ than to the relevant vectors of $(1, 0)$, which are its left and right neighbors on the circle, $\mathcal{R}_{(1,0)} = \{(c_1, s_1), (c_{c-1}, s_{c-1})\} = \{(c_1, s_1), (c_1, -s_1)\}$. Let $\hat{\mathbf{C}}_i$ as in Proposition 11 denote the matrix \mathbf{C}_i reduced to its relevant rows. For the matrix $\hat{\mathbf{D}}_c = \hat{\mathbf{C}}_c \hat{\mathbf{C}}_c^T \in \mathbb{R}^{2 \times 2}$, we therefore obtain:

$$\hat{\mathbf{D}}_c = \begin{bmatrix} 1 - c_1 & 0 - s_1 \\ 1 - c_1 & 0 + s_1 \end{bmatrix} \cdot \begin{bmatrix} 1 - c_1 & 0 - s_1 \\ 1 - c_1 & 0 + s_1 \end{bmatrix}^T = 2(1 - \cos \frac{2\pi}{c}) \cdot \begin{bmatrix} 1 & -c_1 \\ -c_1 & 1 \end{bmatrix}. \quad (33)$$

Due to the spherical/circular symmetry of \mathcal{C} , all matrices $\hat{\mathbf{D}}_i = \hat{\mathbf{C}}_i \hat{\mathbf{C}}_i^T$ are equal to $\hat{\mathbf{D}}_c$. Together with Theorem 10, this leads to the given expression for $\Sigma = \Sigma_1$. \square

Orthant probabilities for general quadrivariate normal distributions are difficult to solve, but for certain specific forms of Σ , explicit formulas for the resulting orthant probabilities in terms of the off-diagonal entries of Σ are known. In the 1960s, Cheng [Che68, Che69] used a clever path integration technique, together with Plackett's reduction formula [Pla54], to ultimately end up with the following expressions for the orthant probabilities for matrices of the above form.

⁷ Note that although the matrices \mathbf{C}_i depend on the absolute positioning of the code words, the dot products $\mathbf{C}_i \mathbf{C}_i^T$ only depends on the relative positions between code words, and is invariant under rotations of \mathcal{C} .

Lemma 2 (Orthant probabilities for a class of quadrivariate normal distributions).

[Che68, Appendix] Let $a, b \in \mathbb{R}$, and let the correlation matrix $\Sigma = \Sigma_{a,b}$ be of the following form:

$$\Sigma = \begin{bmatrix} 1 & a \\ a & 1 \end{bmatrix} \otimes \begin{bmatrix} 1 & b \\ b & 1 \end{bmatrix} = \begin{bmatrix} 1 & a & b & ab \\ a & 1 & ab & b \\ b & ab & 1 & a \\ ab & b & a & 1 \end{bmatrix}. \quad (34)$$

Then the orthant probability $\Phi(a, b) = \Pr_{\mathbf{z} \sim \mathcal{N}(\mathbf{0}, \Sigma)}(\mathbf{z} \geq \mathbf{0})$ for the correlation matrix Σ satisfies:

$$\Phi(a, b) = \frac{1}{16} + \frac{1}{4\pi} (\arcsin a + \arcsin b + \arcsin ab) + \frac{1}{4\pi^2} (\arcsin^2 a + \arcsin^2 b - \arcsin^2 ab). \quad (35)$$

The orthant probability $\Phi(a, b)$ above can be equivalently written in the following form:

$$\Phi(a, b) = \left(\frac{\arccos(-a)}{2\pi} \right)^2 + \left(\frac{\arccos(-b)}{2\pi} \right)^2 - \left(\frac{\arccos(ab)}{2\pi} \right)^2. \quad (36)$$

Note that a, b, ab are the off-diagonal entries of Σ , or equivalently, the arguments of the arccosines $-a, -b, ab$ are the off-diagonal entries of Σ^{-1} , thus showing similarities with the orthant probabilities for 2×2 matrices related to antipodal spherical codes, where $\Phi(a) = \arccos(-a)/(2\pi)$. An interesting open problem, as we will see later, is to establish a pattern in the orthant probabilities for the matrices Σ appearing in Theorem 8 and Corollary 10.

Now, with the above lemma in hand, we are ready to prove Theorem 13.

Proof (Proof of Theorem 13). From Theorem 10, and the observation that regular polygons form isogonal codes on the sphere, we obtain the correlation matrix Σ as described by Lemma 1. Recall that orthant probabilities are invariant under scalar multiplication of the random vector \mathbf{z} ; removing the leading scalar factor of Σ in Lemma 1, the collision probability p_1 remains the same. After removing this factor, we obtain a matrix Σ of the form of Lemma 2, where $a = \cos \theta$ and $b = -\cos \frac{2\pi}{c}$. Through some elementary trigonometric reductions, we then obtain the stated result, where we obtain an additional leading factor c as $\Pr(h(\mathbf{x}) = h(\mathbf{y})) = c \cdot \Pr(h(\mathbf{x}) = h(\mathbf{y}) = 1)$. \square

Let us draw some observations from Theorem 13. First, observe that if we substitute $c = 2$, i.e. using a regular 2-gon, we obtain $p_1 = 1 - \theta/\pi$ and $p_2 = 1/2$, as we expect from Proposition 12. Similarly, substituting $c = 4$ into Theorem 13 we obtain $p_1 = (1 - \theta/\pi)^2$ and $p_2 = (1/2)^2$, matching the combined collision probability of two independent antipodal codes. As the nearest neighbor exponents $\rho = \log p_1 / \log p_2 = \log p_1^2 / \log p_2^2$ are invariant under applying the same exponentiation to both p_1 and p_2 , both the regular 2-gon and 4-gon (square) achieve the same performance when using Gaussian projection matrices \mathbf{A} .

For other values of $c \geq 2$, the collision probabilities do not simplify much further than the given expression in Theorem 13 with c replaced by the corresponding number. Looking at the nearest neighbor exponents $\rho = \log p_1 / \log p_2$ for e.g. $\theta = \frac{\pi}{3}$ and $\theta = \frac{\pi}{4}$, we obtain the two graphs in Figure 5. As we can see, the query exponents for $c = 2$ and $c = 4$ are the same, and using very large polygons does not improve the performance; any polygon with more than 4 vertices achieves worse query exponents ρ than antipodal locality-sensitive hashing. For $c = 3$ however we observe a non-trivial minimum: using equilateral triangles, the query time complexity for nearest neighbor searching is lower than for $c = 2, 4$.

Theorem 14 (In two dimensions, the triangle is optimal). Let $\theta \in (0, \frac{\pi}{2})$. Then, among all project-and-partition hash families induced by two-dimensional isogonal spherical codes, the query exponent $\rho = \log p_1 / \log p_2$ is minimized by the equilateral triangle.

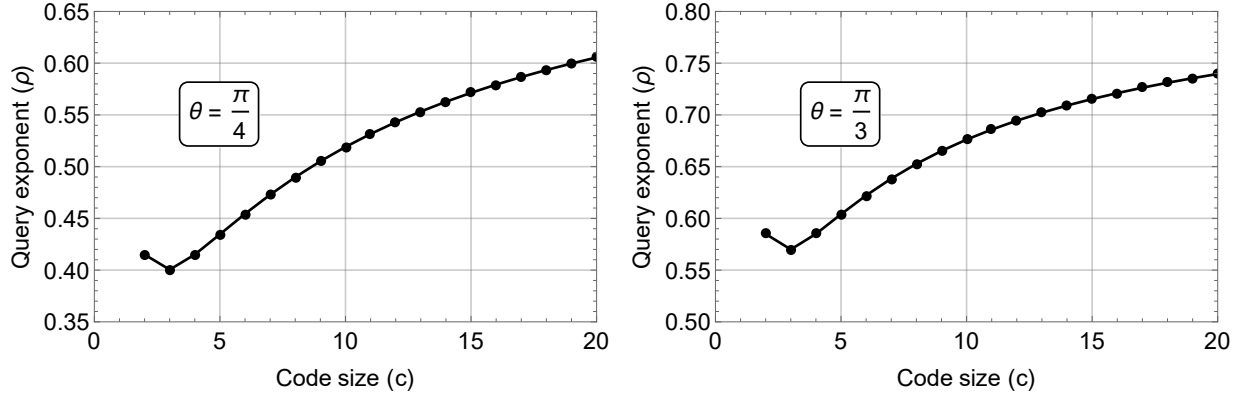


Fig. 5. Query exponents ρ for project-and-partition hash families based on two-dimensional regular polygons. Lower query exponents ρ are better, and the best performance is achieved by the equilateral triangle ($c = 3$). The case $c = 2$ corresponds to hyperplane hashing, while $c = 4$ corresponds to using the vertices from a square, which is asymptotically equivalent to using two (orthogonal) hyperplanes.

Proof. By inspecting the function $f(c, \theta) = \log p_1 / \log p_2$ with p_1 and p_2 as in (31), we see that on the positive reals, its derivative with respect to c always has a single root $c_0 = c_0(\theta) \in (2, 3)$. For $c \leq c_0$ the derivative is negative and for $c \geq c_0$ the derivative is positive, hence on the positive reals, $f(c, \theta)$ is minimized at $c = c_0$, where the exact value c_0 depends on θ . On the natural numbers, $f(c, \theta)$ is therefore minimized either at $c = 2$ or at $c = 3$. Since $f(2, \theta) = f(4, \theta) > f(3, \theta)$, the value at $c = 3$ is the unique global minimum, and therefore for all target nearest neighbor angles $\theta \in (0, \frac{\pi}{2})$, the equilateral triangle achieves the lowest values ρ . \square

For example, when $\theta = \frac{\pi}{3}$ we obtain a query exponent $\rho = 0.56996\dots$ for the equilateral triangle, compared to $\rho = 0.58496\dots$ for the square or for two antipodal points. Recall again that this improvement holds unconditionally, for all d ; these collision probabilities are exact, and do not hide order terms in d . A further overview of query exponents ρ for regular polygons is given in Table 1, in the rows labeled $k = 2$.

5.2 Arbitrary two-dimensional spherical codes

For arbitrary (non-isogonal) two-dimensional spherical codes, where code word \mathbf{c}_i covers a fraction f_i of the circle, the probability that two vectors collide in one of the c hash regions, given their mutual angle θ , can be computed in terms of the vector \mathbf{f} as:

$$p_1(\theta, \mathbf{f}) = \|\mathbf{f}\|_2^2 + c \left(\frac{\pi - \theta}{2\pi} \right)^2 - \frac{1}{4\pi^2} \sum_{i=1}^c \arccos^2(-\cos \theta \cos 2\pi f_i), \quad p_2(\mathbf{f}) = \|\mathbf{f}\|_2^2. \quad (37)$$

The set of query exponents ρ that can be achieved by two-dimensional codes $\mathcal{C} \subset \mathcal{S}^1$ in the project-and-partition framework, given a target angle θ , is then equal to:

$$R_\theta = \left\{ \frac{\log p_1(\theta, \mathbf{f})}{\log p_2(\mathbf{f})} : \mathbf{f} \in \mathbb{R}^c, c \geq 2, \mathbf{f} \geq \mathbf{0}, \|\mathbf{f}\|_1 = 1 \right\}. \quad (38)$$

Here $\|\mathbf{f}\|_2$ and $\|\mathbf{f}\|_1$ denote the ℓ_2 -norm and ℓ_1 -norm of \mathbf{f} . Although a numerical evaluation indicates that, for arbitrary $\theta \in (0, \frac{\pi}{2})$, the minimum over R_θ is obtained for $\mathbf{f} = (\frac{1}{3}, \frac{1}{3}, \frac{1}{3})$, we leave a formal proof of the optimality of the equilateral triangle over all two-dimensional codes as an open problem.

6 Three-dimensional codes

As the dimensionality increases, the dimensions of the matrices \mathbf{C}_i in Theorem 8 and Corollary 10 generally also increase, even when using the relevant vectors optimization of Proposition 11. In particular, as each Voronoi region in three dimensions is defined by at least three relevant vectors, the matrix Σ will be at least six-dimensional with non-trivial off-diagonal entries. The bad news is that for none of the three-dimensional codes we considered, we could derive analytic, closed-form expressions for the collision probabilities; numerical integration seems to be necessary to evaluate their performance. The good news however is that Section 3 provides us with a computational framework to evaluate the suitability of a spherical code for nearest neighbor searching, given the vertices defining the spherical code.

Table 1 summarizes the results of a brief survey of various spherical codes appearing in the literature in different contexts. The three-dimensional codes are given in the rows labeled $k = 3$. The codes we considered and evaluated numerically are:

- The **tetrahedron**, or the 3-simplex, consisting of 4 equidistributed points on the sphere;
- The **octahedron**, or the 3-orthoplex (cross-polytope), consisting of the 6 unit vectors $\pm \mathbf{e}_i$;
- The **cube**, consisting of 8 vertices of the form $\frac{1}{3}\sqrt{3} \cdot (\pm 1, \pm 1, \pm 1)$;
- The **icosahedron**, one of the five Platonic solids, with 12 vertices;
- The **cuboctahedron**, the vertex figure of the root lattices A_3 and D_3 , with 12 vertices;
- The **dodecahedron**, the largest of the Platonic solids, with 20 vertices;
- Three **sphere packings** of 5, 7, 9 vertices from the sphere packing database of Sloane [Slo].

Numerically evaluating the resulting query exponents ρ , it seems that for all $\theta \in (0, \frac{\pi}{2})$, the tetrahedron gives the best query exponents ρ . Similar to the two-dimensional case, using large, dense spherical codes does not seem to help; a fine-grained partition may make p_2 smaller, but at the same time p_1 then also becomes so much smaller that ρ still increases. Note that, similar to the triangle, the tetrahedron belongs to the class of simplices.

Conjecture 15 (In three dimensions, the tetrahedron is optimal) *Let $\theta \in (0, \frac{\pi}{2})$. Then, among all project-and-partition hash families induced by three-dimensional (isogonal) spherical codes, the query exponent $\rho = \log p_1 / \log p_2$ is minimized by the regular tetrahedron.*

For the tetrahedron, the collision probabilities are $p_2 = 1/4$ and:

$$p_1 = 4 \cdot \Pr_{z \sim \mathcal{N}(\mathbf{0}, \Sigma)}(z \geq \mathbf{0}), \quad \Sigma = \begin{bmatrix} 1 & \cos \theta \\ \cos \theta & 1 \end{bmatrix} \otimes \begin{bmatrix} 1 & 1/2 & 1/2 \\ 1/2 & 1 & 1/2 \\ 1/2 & 1/2 & 1 \end{bmatrix}. \quad (39)$$

A further simplification of p_1 , i.e. finding a closed-form expression for this six-dimensional orthant probability is left as an open problem [Laa19].

For numerically computing the values ρ in Table 1 for three-dimensional codes, we used the statistical software R together with the mvtnorm-package [GBM⁺19], which specifically implements fast and precise evaluation of orthant probabilities. For instance, for the tetrahedron with $\theta = \frac{\pi}{3}$, we numerically compute $\rho = 0.559998$. Using an independent C implementation, we performed Monte Carlo experiments, which for $\theta = \frac{\pi}{3}$ led to the estimate $\rho = 0.559997$ based on 10^8 random trials.

Note that the (numerical) integration task becomes more complex, and likely less precise, as the dimensionality of the problem increases (i.e. the size of Σ increases). For isogonal codes, the dimensions of Σ are not determined by the size of the code but by the number of relevant vectors for each code word. The entries in Table 1 may therefore be less precise for e.g. the icosahedron, with $|\mathcal{R}| = 5$, and for large irregular sphere packings from [Slo].

7 Four-dimensional codes

As for the three-dimensional case, the orthant probabilities in the four-dimensional case generally appear too hard to evaluate analytically. Instead, we numerically computed parameters ρ for different angles θ for the following list of four-dimensional spherical codes, by estimating the corresponding multivariate integrals with the R-library [GBM⁺19]:

- The **pentatope** or **5-cell**, also known as the 4-simplex, with 5 vertices;
- The **16-cell**, the four-dimensional version of the orthoplex, with 8 vertices;
- The **tesseract**, or the four-dimensional hypercube, with 16 vertices;
- The **octacube** or **24-cell**, the vertex figure of the D_4 root lattice, with 24 vertices;
- The runcinated 5-cell, corresponding to the 20 roots of the A_4 -lattice;
- Four **sphere packings** of 6, 7, 10, 13 vertices from the sphere packing database of Sloane [Slo].

The only other regular convex polytopes not mentioned above are the 120-cell and 600-cell which, as their names suggest, are rather large; not only will the numerical evaluation (or Monte Carlo estimation) of the corresponding orthant probabilities likely be imprecise, but we also expect that such large codes are unlikely to offer an improvement, if we extrapolate the intuition obtained from the results in two and three dimensions to the four-dimensional setting.

As shown in Table 1, an interesting phenomenon occurs in dimension 4. For two- and three-dimensional spherical codes we saw that the simplices give the best performance, beating other codes such as the orthoplices. In four dimensions however, for small angles θ , the more fine-grained partitioning offered by the orthoplex gives a better performance for the associated locality-sensitive hashing scheme. Note that the best parameters ρ are achieved by the simplex and orthoplex; these polytopes seem well-suited for locality-sensitive hashing, and even the nicest other spherical codes cannot compete with these highly regular and symmetric shapes.

Conjecture 16 (In four dimensions, the 5-cell and 16-cell are optimal) *Let $\theta \in (0, \frac{\pi}{2})$.*

There exists a parameter $\theta_0 \in (0, \frac{\pi}{2})$ such that, among all project-and-partition hash families induced by four-dimensional (isogonal) spherical codes, the query exponent ρ is minimized by:

- *the 16-cell, if $\theta \in (0, \theta_0)$;*
- *the 5-cell, if $\theta \in (\theta_0, \frac{\pi}{2})$.*

Numerically, we estimate the cross-over point between the 5-cell and 16-cell in terms of the query exponent ρ to lie at $\theta_0 \approx 0.33\pi$, slightly below $\theta = \frac{\pi}{3}$. See also Figure 1, showing the improvements over hyperplane hashing for both the 5-cell and the 16-cell, and showing that the cross-over point between both four-dimensional codes lies close to $\theta = \frac{\pi}{3}$. From a practical point of view however, as discussed in Section 10, using larger spherical codes (in a fixed dimension) is generally better, as the hash computations are then cheaper. In that sense, using the 16-cell may be a better choice than using a 5-cell for partitions even for angles $\theta > \theta_0$.

For completeness, both for the 5-cell and 16-cell we also performed independent Monte Carlo estimations of the collision probabilities using 10^8 trials for each value θ in Table 1, to verify that these numbers are accurate. The first three decimals in Table 1 were always an exact match, and only small deviations in the fourth decimal were occasionally observed in the regime of small θ .

Again, we stress that the list of spherical codes given in Table 1 is by no means exhaustive, and the framework provided in Section 3 may be useful for evaluating any other spherical codes, if one suspects better spherical codes exist for partitioning the space.

8 Higher-dimensional codes

For high dimensions k , the orthant probabilities become increasingly difficult to evaluate, and the number of known, *nice* spherical codes quickly decreases. A well-known result is that in five or more dimensions, there exist only three classes of regular convex polytopes, which have also been studied before in the context of locality-sensitive hashing [TT07, TT09, AIL⁺15, Laa17, KW17]. These are the simplices, orthoplices, and hypercubes. Besides these families of polytopes, we will also study the families of expanded simplices and rectified orthoplices, which correspond to the vertex figures of the A_k and D_k root lattices. Together with these families, we further study three more special polytopes in five and six dimensions, listed in Table 1:

- The **1₂₁-polytope** or the 5-demicube, obtained by taking 16 vertices of the 5-cube;⁸
- The **1₃₁-polytope**, or the 6-dimensional demicube on 32 vertices;
- The **2₂₁-polytope** or **Schäfli polytope** on 27 vertices, with symmetries of the E_6 lattice.

The other polytopes in Table 1 for dimensions higher than four are all from the families S_k , O_k , C_k , A_k and D_k which we further discuss separately below.

8.1 Simplices (S_k)

Recall that simplices can most easily be described as the subset in \mathbb{R}^{k+1} containing all standard unit vectors $\mathbf{e}_1, \dots, \mathbf{e}_{k+1}$. We are unable to obtain closed-form expressions for p_1 and ρ for $k \geq 3$, beyond the multivariate integral representation from Corollary 10, and we only obtain a closed-form expression of the correlation matrices appearing in the computation of p_1 below. In this case the matrix $\mathbf{D} \in \mathbb{R}^{k \times k}$ has the simple shape of having ones on the diagonal and all off-diagonal entries being equal to $1/2$. (Observe that orthant probabilities for such matrices, with all off-diagonal entries equal to the same value, were studied in e.g. [Ste62].) Yet, due to the Kronecker product, an exact evaluation of the resulting orthant probabilities for $k \geq 3$ seems difficult. In the following proposition, recall that \mathbf{I}_k denotes the identity matrix, and \mathbf{J}_k the all-1 matrix.

Proposition 17 (Collision probabilities for simplices) *Let $\mathcal{C} \subset \mathcal{S}^{k-1}$ consist of the $k+1$ vertices of the simplex, and let $\theta \in (0, \frac{\pi}{2})$. Then the corresponding project-and-partition hash family \mathcal{H} is (θ, p_1, p_2) -sensitive, with $p_2 = 1/(k+1)$ and:*

$$p_1 = (k+1) \cdot \Pr_{\mathbf{z} \sim \mathcal{N}(\mathbf{0}, \Sigma)}(\mathbf{z} \geq \mathbf{0}), \quad \Sigma = \begin{bmatrix} 1 & \cos \theta \\ \cos \theta & 1 \end{bmatrix} \otimes \frac{1}{2}(\mathbf{J}_k + \mathbf{I}_k). \quad (40)$$

Proof. For ease of computations, let $\mathcal{C} = \{\mathbf{e}_i : i = 1, \dots, k+1\}$. Although this code is not centered around the origin, and lies in \mathbb{R}^{k+1} rather than \mathbb{R}^k , none of these things matter when computing $\mathbf{D} = \hat{\mathbf{C}}_i \hat{\mathbf{C}}_i^T$, which is a function only of the difference vectors $\mathbf{c}_i - \mathbf{c}_j$. Now, a vector lies in the Voronoi cell of the vertex \mathbf{e}_1 if and only if it lies closer to \mathbf{e}_1 than to all its neighbors, which in this case are all other vectors in the code. The difference vectors $\mathbf{e}_1 - \mathbf{e}_j$ all have norm $\sqrt{2}$ and pairwise inner products 1, hence after dividing \mathbf{D} by 2 we obtain a matrix with ones on the diagonal and $1/2$ everywhere off the diagonal. The result then follows from Theorem 10. \square

Asymptotically, as $d \rightarrow \infty$, using simplices is equivalent to using cross-polytopes, and the last rows of Table 1 illustrate this asymptotic scaling as k increases.

⁸ Viewing the hypercube as a bipartite graph, the vertices of the demicube are all vertices from one of the two sets.

8.2 Orthoplices (\mathcal{O}_k)

For cross-polytopes or orthoplices, consisting of the $2k$ code words $\pm e_1, \dots, \pm e_k$, unfortunately we also cannot easily derive an analytic expression for the collision probabilities for $k \geq 3$. We state the reduced form of the correlation matrix below, where the matrix $\mathbf{D} \in \mathbb{R}^{(2k-2) \times (2k-2)}$ is a Toeplitz matrix with ones on the diagonal, $1/2$ on most of the other diagonals, and one diagonal strip above and below the diagonal with all zeros.

Proposition 18 (Collision probabilities for orthoplices) *Let $\mathcal{C} \subset \mathcal{S}^{k-1}$ consist of the $2k$ vertices of the orthoplex, and let $\theta \in (0, \frac{\pi}{2})$. Then the corresponding project-and-partition hash family \mathcal{H} is (θ, p_1, p_2) -sensitive, with $p_2 = 1/(2k)$ and:*

$$p_1 = 2k \cdot \Pr_{z \sim \mathcal{N}(\mathbf{0}, \Sigma)}(z \geq \mathbf{0}), \quad \Sigma = \begin{bmatrix} 1 & \cos \theta \\ \cos \theta & 1 \end{bmatrix} \otimes \frac{1}{2} \begin{bmatrix} \mathbf{J}_{k-1} + \mathbf{I}_{k-1} & \mathbf{J}_{k-1} - \mathbf{I}_{k-1} \\ \mathbf{J}_{k-1} - \mathbf{I}_{k-1} & \mathbf{J}_{k-1} + \mathbf{I}_{k-1} \end{bmatrix}. \quad (41)$$

Proof. Without loss of generality, let $\mathcal{C} = \{\pm e_j : j = 1, \dots, k\}$. For the vector $\mathbf{c}_1 = e_1$, the relevant vectors are $\mathcal{R}_1 = \mathcal{C} \setminus \{\pm e_1\}$, and taking differences with the relevant vectors, we observe that the matrix $\hat{\mathbf{C}}_1$ has $2k - 2$ rows $e_1 \pm e_j$, for $j = 2, \dots, k$. For the product $\mathbf{D} = \hat{\mathbf{C}}_1 \hat{\mathbf{C}}_1^T$ we get twos on the diagonal, ones for most off-diagonal entries, and each row is paired up with exactly one other row whose joint correlation is 0. Through a suitable reordering of the rows/columns of \mathbf{D} , we thus get the claimed shape of \mathbf{D} . Finally, with \mathcal{C} being isogonal and of size $2k$, using Theorem 10 we get the claimed expressions for p_1 and p_2 . \square

As $k \rightarrow \infty$, from [AIL⁺15] we know that the parameters ρ scale optimally as $\rho \rightarrow 1/(2c^2 - 1)$, where $c = \sqrt{1/(1 - \cos \theta)}$ is the approximation factor for worst-case approximate nearest neighbor searching. Substituting values $\theta \in \frac{\pi}{12}\{1, 2, 3, 4, 5\}$, we obtain the values in the bottom rows of Table 1.

8.3 Hypercubes (\mathcal{C}_k)

The easiest of these three families of convex regular polytopes to analyze is the family of hypercubes. For arbitrary $k \geq 1$, these codes consist of 2^k vertices of the form $\frac{1}{\sqrt{k}}(\pm e_1 \pm \dots \pm e_k)$. When using normal matrices $\mathbf{A} \sim \mathcal{N}(0, 1)^{k \times d}$ to project down onto a k -dimensional subspace, the following proposition shows that the query exponent does not change at all as k increases.

Proposition 19 (Collision probabilities for hypercubes) *Let $\mathcal{C} \subset \mathcal{S}^{k-1}$ consist of the 2^k vertices of the hypercube, and let $\theta \in (0, \frac{\pi}{2})$. Then the corresponding project-and-partition hash family \mathcal{H} is (θ, p_1, p_2) -sensitive, with:*

$$p_1 = \left(1 - \frac{\theta}{\pi}\right)^k, \quad p_2 = \left(\frac{1}{2}\right)^k. \quad (42)$$

As a result, when using Gaussian projection matrices \mathbf{A} the query exponents ρ for hypercubes are equal to those for the antipodal spherical code of Proposition 12.

Proof. As before, scaling \mathcal{C} by a constant factor does not affect collision probabilities, so w.l.o.g. we may let \mathcal{C} consist of the 2^k vectors $(\pm 1, \pm 1, \dots, \pm 1)$. A vector \mathbf{x} is mapped to the code word $\mathbf{c}_0 = (1, 1, \dots, 1)$ if and only if it is closer to this code word than to its relevant vectors \mathcal{R}_0 , which in this case are the vectors with $(k - 1)$ entries equal to $+1$ and one entry equal to -1 . For $j = 1, \dots, k$ let us denote by \mathbf{c}_j the vector with ones everywhere, except at position j where we have a -1 .

For the difference vectors $\mathbf{c}_0 - \mathbf{c}_j$ with $\mathbf{c}_j \in \mathcal{R}_1$ we get $\mathbf{c}_0 - \mathbf{c}_j = 2\mathbf{e}_j$, and as a result we obtain $\hat{\mathbf{C}}_0 \hat{\mathbf{C}}_0^T = 4 \cdot \mathbf{I}_k$, which is a scalar multiple of the identity matrix. Now, note that a correlation matrix \mathbf{I}_k essentially means that the entries of the random vector are independent. It is therefore an easy exercise to see that, for all matrices \mathbf{A} :

$$\Pr_{z \sim \mathcal{N}(\mathbf{0}, \mathbf{A} \otimes \mathbf{I}_k)}(\mathbf{z} \geq \mathbf{0}) = \Pr_{z \sim \mathcal{N}(\mathbf{0}, \mathbf{I}_k \otimes \mathbf{A})}(\mathbf{z} \geq \mathbf{0}) = \Pr_{z \sim \mathcal{N}(\mathbf{0}, \mathbf{A})}(\mathbf{z} \geq \mathbf{0})^k. \quad (43)$$

Together with the derivation of the orthant probability for the one-dimensional antipodal spherical code, this leads to $p_1 = 2^k \cdot (\pi - \theta)^k / (2\pi)^k = (1 - \theta/\pi)^k$. As \mathcal{C} is isogonal, we further obtain $p_2 = 1/2^k$ as claimed. \square

Note that the paper [Laa17] showed that, if $\mathbf{A} \in \mathbb{R}^{d \times d}$ is chosen as a random *orthogonal* matrix, then in fact the performance of hypercube hashing gets better as k increases. Here however we assumed $\mathbf{A} \sim \mathcal{N}(0, 1)^{k \times d}$, which for small k is essentially equivalent to sampling \mathbf{A} as an orthogonal matrix, but is not quite the same for large k ; see e.g. [DF87, Jia06] for more details on how the gap between orthogonal and Gaussian matrices changes with the relation between k and d . This leads to two different asymptotic scalings, as indicated in the bottom rows of Table 1.

8.4 Expanded simplices (A_k)

Similar to simplices, so-called expanded simplices (the vertex figures of the A_k root lattices) can most easily be described as a subset in \mathbb{R}^{k+1} . These spherical codes contain all differences between unit vectors, $\mathbf{e}_i - \mathbf{e}_j$ for $i \neq j$. These vertices all lie on a k -dimensional hyperplane, and can thus be viewed as a k -dimensional spherical code. For these codes the matrix $\mathbf{D} \in \mathbb{R}^{(2k-1) \times (2k-1)}$ has a block structure described below.

Proposition 20 (Collision probabilities for expanded simplices) *Let $\mathcal{C} \subset \mathcal{S}^{k-1}$ consist of the $k(k+1)$ vertices of the expanded simplex, and let $\theta \in (0, \frac{\pi}{2})$. Then the corresponding project-and-partition hash family \mathcal{H} is (θ, p_1, p_2) -sensitive, with $p_2 = 1/k(k+1)$ and:*

$$p_1 = k(k+1) \cdot \Pr_{z \sim \mathcal{N}(\mathbf{0}, \Sigma)}(\mathbf{z} \geq \mathbf{0}), \quad \Sigma = \begin{bmatrix} 1 & \cos \theta \\ \cos \theta & 1 \end{bmatrix} \otimes \frac{1}{2} \begin{bmatrix} \mathbf{J}_{k-1} + \mathbf{I}_{k-1} & -\mathbf{I}_{k-1} \\ -\mathbf{I}_{k-1} & \mathbf{J}_{k-1} + \mathbf{I}_{k-1} \end{bmatrix}. \quad (44)$$

We omit the proof, which is analogous to the proofs of Propositions 17 and 18.

Observe that, as hashing in the expanded simplex corresponds to mapping to the two largest coordinates of a vector, for large d up to order terms this is essentially equivalent to using two independent simplex hashes. For expanded simplices we therefore again get the optimal scaling for large k also obtained with orthoplices and simplices, as illustrated in Table 1.

8.5 Rectified orthoplices (D_k)

Rectified orthoplices, related to the root lattices D_k , contain as vertices all pairwise combinations of unit vectors; in contrast to A_k , where the signs must be opposite, here any combination of signs is included. As a subset of \mathbb{R}^k , this code thus contains the $2k(k-1)$ vertices of the form $\pm \mathbf{e}_i \pm \mathbf{e}_j$ for $i \neq j$. For these codes the matrix $\mathbf{D} \in \mathbb{R}^{(2k-1) \times (2k-1)}$ has a 2×2 block structure described below.

Proposition 21 (Collision probabilities for rectified orthoplices) *Let $\mathcal{C} \subset \mathcal{S}^{k-1}$ consist of the $2k(k-1)$ vertices of the rectified orthoplex, and let $\theta \in (0, \frac{\pi}{2})$. Then the corresponding project-and-partition hash family \mathcal{H} is (θ, p_1, p_2) -sensitive, with $p_2 = 1/2k(k-1)$ and:*

$$p_1 = 2k(k-1) \cdot \Pr_{z \sim \mathcal{N}(\mathbf{0}, \Sigma)}(z \geq \mathbf{0}), \quad \Sigma = \begin{bmatrix} 1 & \cos \theta \\ \cos \theta & 1 \end{bmatrix} \otimes \frac{1}{2} \begin{bmatrix} \mathbf{J} + \mathbf{I} & \mathbf{J} - \mathbf{I} & \mathbf{I} & -\mathbf{I} \\ \mathbf{J} - \mathbf{I} & \mathbf{J} + \mathbf{I} & -\mathbf{I} & \mathbf{I} \\ \mathbf{I} & -\mathbf{I} & \mathbf{J} + \mathbf{I} & \mathbf{J} - \mathbf{I} \\ -\mathbf{I} & \mathbf{I} & \mathbf{J} - \mathbf{I} & \mathbf{J} + \mathbf{I} \end{bmatrix}. \quad (45)$$

All matrices $\mathbf{I} = \mathbf{I}_{k-2}$ and $\mathbf{J} = \mathbf{J}_{k-2}$ above are square matrices of size $(k-2) \times (k-2)$.

We omit the proof, which is analogous to the proofs of Propositions 17 and 18. Note again that, as we are mapping to the two largest coordinates after projection, the hash function for the rectified orthoplex has the same asymptotic scaling as the simplex and orthoplex.

8.6 Comparison

To compare these families of spherical codes in terms of their performance for nearest neighbor searching, Figure 2 depicts the resulting parameters ρ for different values k , focusing on the two cases $\theta = \frac{\pi}{3}$ and $\theta = \frac{\pi}{4}$. As observed previously there is a cross-over between simplices and orthoplices around $k = 4$, after which the orthoplex consistently performs better than the simplex. The hypercube, as shown in Proposition 19, remains stable at the same performance as the antipodal code, regardless of the choice of dimension k .

9 Utopian spherical cap estimates

To get an idea how good the spherical codes considered above are, ideally we would find a matching lower bound, stating that any spherical code of dimension at most k must satisfy $\rho(\theta) \geq \rho_k(\theta)$, for some monotonically increasing function $\rho_k : (0, \frac{\pi}{2}) \rightarrow (0, 1)$. However, ruling out the existence of exotic spherical codes which happen to perform better than the ones we considered seems difficult.

As has been observed several times before [AINR14, BDGL16, ALRW17], using spherical caps to partition the sphere into regions seems to work best, so that the regions have nice, symmetric shapes that ultimately seem to minimize the exponent ρ . We can therefore get (conjectured) lower bounds on the parameter ρ by assuming that the sphere can be perfectly divided into an integer number of spherical caps, and estimating the resulting parameter ρ for these utopian⁹ partitions of the sphere. This leads to the following conjecture, where we assume such perfect spherical cap partitions exist, and where we compute collision probabilities p_1, p_2 and the query exponents ρ accordingly.

Conjecture 22 (Spherical cap lower bounds) *Let $\mathcal{C} \subset \mathcal{S}^{k-1}$ be a spherical code, and let \mathcal{H} be the associated project-and-partition hash family. Then the parameter ρ for \mathcal{C} , for angle $\theta \in (0, \frac{\pi}{2})$, must satisfy:*

$$\rho(\theta) \geq \rho_k(\theta) := \min_{c \geq 2} \rho_k(c, \theta), \quad (46)$$

⁹ Note that for $k \geq 3$ it is impossible to partition the sphere into spherical caps, as regions either overlap, or part of the sphere remains uncovered. These conjectured lower bounds therefore do not correspond to actual, achievable bounds, and are likely not tight.

where $\rho_k(c, \theta)$ is given by:

$$\rho_k(c, \theta) := \log \left\{ \Pr_{\mathbf{x}, \mathbf{y} \sim \mathcal{N}(0,1)^k} \left(\frac{x_1}{\|\mathbf{x}\|} \geq \alpha_k(c), \frac{x_1 \cos \theta + y_1 \sin \theta}{\|\mathbf{x} \cos \theta + \mathbf{y} \sin \theta\|} \geq \alpha_k(c) \right) \right\} / \log \left(\frac{1}{c} \right), \quad (47)$$

and $\alpha_k(c)$ is the solution to $\frac{1}{2} \cdot I_{1-\alpha^2}(\frac{k-1}{2}, \frac{1}{2}) = \frac{1}{c}$.

Here $\alpha_k(c)$ is the spherical cap height α such that $\mu(\mathcal{C}_\alpha)/\mu(\mathcal{S}^{k-1}) = 1/c$, so that volume-wise, c such caps could perfectly cover the k -dimensional unit sphere. The exponent $\rho_k(c)$ is then the ratio of the logarithms of the collision probabilities p_1 and p_2 , assuming such an isogonal code with spherical cap regions exists, and by minimizing over the code size c we conjecture this leads to an absolute lower bound on ρ for any code on the k -sphere. Note that by fixing both k and c , we can similarly obtain a (conjectured) lower bound on the performance of any k -dimensional code of cardinality c .

For analyzing actual spherical codes, we obtained conditions of the form $\|\mathbf{x} - \mathbf{c}_i\| \geq \|\mathbf{x} - \mathbf{c}_j\|$, which then translated to conditions $\langle \mathbf{x}, \mathbf{c}_i - \mathbf{c}_j \rangle \geq 0$, leading to orthant probabilities. Here however we have different conditions of the form $\|\mathbf{x}/\|\mathbf{x}\| - \mathbf{c}_i\| \leq u$ for \mathbf{x} to be contained in the Voronoi cell (spherical cap) defined by code word \mathbf{c}_i . Assuming w.l.o.g. $\mathbf{c} = \mathbf{e}_1$, the formulas reduce to those given in (47), but these cannot be expressed in terms of orthant probabilities.

For small values $k = 1, \dots, 6$, and for the angles $\theta \in \frac{\pi}{12}\{1, \dots, 5\}$, we numerically computed values $\rho_k(c, \theta)$, and taking the minimum over c , we obtained the values $\rho_k(\theta)$ given in Table 1. The superscripts in Table 1 indicate the value c leading to the minimum value ρ , i.e. the ideal code size for these utopian spherical cap codes. Although these codes are not actually instantiable, these conjectured lower bounds may be useful as a guideline for choosing the code size c , when trying to come up with the best spherical codes in this framework.

From Table 1, observe that as the angle θ decreases, and the nearest neighbor is expected to lie very close to the query vector, the optimal code size c increases; for problem instances where the neighbor lies very close to the query vector, a fine-grained partition will likely work better. Also note that as k increases, the optimal code size c for these utopian codes increases as well, and whereas for small k the optimal code size is always less than the number of vertices of the simplex and orthoplex, for larger k the optimal code size increases beyond that of the simplex, and also beyond that of the orthoplex. This is in line with our observation that as k increases, orthoplices start outperforming simplices, and this also hints at the idea that as k increases further, even denser codes (likely with a superlinear number of vertices) will exhibit a better performance (smaller query exponents ρ) than partitions based on the cross-polytopes.

Conjecture 23 (Orthoplices are not optimal for large k) *There exists a dimension $k_0 \in \mathbb{N}$ such that, for all dimensions $k \geq k_0$, there exist spherical codes $\mathcal{C} \subset \mathcal{S}^{k-1}$ whose query exponents ρ in the project-and-partition framework are smaller than the exponents ρ of the k -orthoplex.*

An interesting open question, which may well be closely related to other sphere packing and covering problems, is to find higher-dimensional spherical codes that are more suitable for nearest neighbor tasks than using the vertices of simplices or orthoplices.

10 Choosing a code in practice

With the above framework in mind, and looking at the results from Table 1 and Figures 1 and 2, one might ask: how do I choose the best spherical code for my application? Is this purely a matter of choosing the code with the smallest exponent ρ ? Or is the practical performance affected by other aspects of the code as well?

To look for an answer to this question, recall that in locality-sensitive hashing (as in Equation (9)) there are several parameters that play a role:

$$\rho = \frac{\log 1/p_1}{\log 1/p_2}, \quad \ell = \frac{\log n}{\log 1/p_2}, \quad t = O(n^\rho). \quad (48)$$

Here the constant in t determines the success probability of the scheme. Now, the concrete costs for finding nearest neighbors with locality-sensitive hashing can be summarized as follows:

Projections: For a k -dimensional code, we use Gaussian projection matrices $\mathbf{A} \sim \mathcal{N}(0, 1)^{k \times d}$, and without further optimizations to \mathbf{A} , computing a product $\mathbf{A}\mathbf{x}$ requires $k \cdot d$ multiplications. Generating such a matrix \mathbf{A} can also be done in time proportional to $k \cdot d$.

Decoding: Although for some spherical codes faster decoding algorithms may exist, in general the decoding cost for a spherical code of size c in dimension k is proportional to $k \cdot c$ multiplications.

Hash tables: We need $t = O(n^\rho)$ hash tables for our data structure.

Hash functions: For each of the t tables, we need to initialize ℓ random hash functions, for a cost of $\ell \cdot t$ hash functions. Each of these requires initializing a random projection matrix $\mathbf{A} \sim \mathcal{N}(0, 1)^{k \times d}$, which can all be generated in time proportional to $\ell \cdot t \cdot k \cdot d$ multiplications.

Preprocessing time: For each of n vectors, and each of t hash tables, we need to compute the k -concatenated hash value, and insert the vector in the corresponding bucket. Timewise, computing all hash values for all vectors takes time proportional to $\ell \cdot t \cdot k \cdot d \cdot n$.

Memory requirement: We need to store t hash tables, each of which contains all n vectors, for a total cost of $t \cdot n$ entries in the hash tables.¹⁰

Query time – Hashing: Given a vector, we need to compute its hash values in all t hash tables, for a cost of $\ell \cdot t \cdot k \cdot d$ multiplications.

Query time – Comparisons: In total we expect that, apart from the nearest neighbor, approximately t vectors will collide with a query vector in the t hash tables. Going through these vectors to find the actual nearest neighbor can be done in time proportional to $t \cdot d$.

Here, an important observation is that the projections generally become more costly as the dimension k of the spherical code increases; in higher dimensions, spherical codes with better parameters ρ exist, but at the same time we pay for these more complex spherical codes in the decoding costs. The highest time and space complexities for the different parts of the nearest neighbor data structure can be summarized as follows:

$$T_{\text{query}} = O(\ell \cdot t \cdot k \cdot d), \quad T_{\text{preprocessing}} = O(n \cdot T_{\text{query}}), \quad S = O(t \cdot n), \quad (49)$$

For the query time complexity T_{query} , the factor d is constant and does not depend on the choice of the spherical code \mathcal{C} . Similarly, the term ℓ contains a factor $\log n$ which does not depend on the choice of \mathcal{C} . Dividing out a factor $n \log_2 n$, the product $t \cdot \ell \cdot k / \log_2 n$ has the following form for isogonal codes \mathcal{C} :

$$\frac{t \cdot \ell \cdot k}{\log_2 n} = O\left(n^\rho \cdot \frac{k}{\log_2 c}\right). \quad (50)$$

Now, for large n this product is clearly minimized especially when ρ is smallest. For concrete values of n however, the other main factor that determines the query complexity is the ratio $\log_2(c)/k$. Here $\log_2(c)$ can be seen as the number of hash bits that are extracted from a single

¹⁰ Observe that we can keep a single copy of the entire list in memory, and only store pointers of essentially constant space to these vectors in the hash tables.

hash value $h(\mathbf{x}) \in \{1, \dots, c\}$, while the factor k comes from the cost of computing a projection onto a k -dimensional subspace. In general, codes with a large ratio $\log_2(c)/k$ require fewer random projections to extract the necessary number of hash bits to determine the hash bucket, while small codes in high dimensions are in that sense rather costly. This quantitatively explains why e.g. hyperplane hashing is fast in practice, as $\log_2(c)/k = 1$, but cross-polytope hashing has a high cost for computing projections, as $\log_2(c)/k = O(\log(k)/k)$ is almost a linear factor smaller.

To compare all codes in terms of their extracted number of bits per projection, as well as their query exponents ρ , Figure 3 shows the resulting trade-offs for the spherical codes considered in this paper. As we can see, there is often a concrete trade-off between the query exponent ρ and the ratio of extracted hash bits $\log_2(c)/k$; codes with small ρ generally have a high hash cost, and codes which partition a low-dimensional space in many regions pay the price with a higher value ρ . Figure 3 also paints a different picture as to which codes are best suited in practice, compared to Table 1; the lattice-based codes D_k may be better choices in practice than the pure orthoplex hashing of [AIL⁺15], achieving better values ρ while keeping the extracted hash bits per projection vector larger than for orthoplex hashing.

For an even more concrete comparison of different codes in practice, Figure 4 describes concrete cost estimates for processing queries for different spherical codes, for different parameters n . Here the query cost estimate is simplified to $t \cdot \ell \cdot k \cdot d$, without taking into account further multiplicative order terms (which are likely to be roughly the same for different spherical codes). As the figure shows, for large n the query exponent ρ dominates, and codes with small values ρ achieve the best query cost estimates. For smaller n (e.g. $n = 10^5$, which might be the size of the database in applications in cryptanalysis [Laa15, BDGL16]), the cross-over point with hyperplane hashing quickly goes down, and using full-size cross-polytopes may not be as practical as using hyperplanes to partition the space; the smaller ρ of cross-polytope hashing does not outweigh the higher cost of the many random projections. This matches practical results from e.g. [Laa15, BL16, BDGL16, MLB15, MLB17], which established that in applications with rather small n , hyperplane hashing dominates. For other applications, where n is larger, using D_k lattices or e.g. the 2_{21} -polytope seems to give the best performance.

As a generalization of the (rectified) orthoplex families of hash functions O_k and D_k , we finally propose the following hash function families, mapping a vector to the m absolute largest coordinates.

Definition 24 (m -max locality-sensitive hash functions) *Let $1 \leq m \leq k \leq d$. Then we define the m -max hash function family \mathcal{H} as the project-and-partition hash family with code:*

$$\mathcal{C} = \left\{ \sum_{i=1}^k s_i \mathbf{e}_i : \mathbf{s} \in \{-1, 0, 1\}^k, \|\mathbf{s}\|_1 = m \right\}. \quad (51)$$

For arbitrary k and m , this spherical code has size $c = 2^m \binom{k}{m}$.

As special cases, $m = 1$ corresponds to orthoplex hashing (O_k), $m = 2$ corresponds to the rectified orthoplices (D_k), and $m = k$ corresponds to hypercube hashing (C_k). As Figure 3 suggests that larger codes ($m = 2$) may work better in practice than smaller codes ($m = 1$), we predict that for large k , larger values m will outperform both orthoplex hashing and rectified orthoplex hashing. An interesting open question would be to estimate how m should ideally scale with k to obtain the best results in practice.

11 Discussion

With the project-and-partition framework outlined in Section 3, we can now easily formalize and analyze the performance of any spherical code in this framework, and analyze the collision probabilities and query exponents either analytically (by attempting to simplify the corresponding orthant probabilities) or numerically (by evaluating these multivariate integrals with mathematical software). We observed that already in two dimensions, it is possible to improve upon hyperplane hashing by using triangular partitions, and we described closed-form formulas for the collision probabilities for triangular hashing, as well as for arbitrary k -gon partitions.

For $k = 3$ the tetrahedron seems optimal, while for larger k the simplices are overtaken by orthoplices in terms of their performance. Although our analysis is not quite equivalent to using full-dimensional orthoplices with orthogonal rotation matrices (as we analyze using Gaussian projection matrices \mathbf{A}), this does make a solid case for the use of orthoplices, as advertised in [TT07, TT09, AIL⁺15, KW17], and observed in nearest neighbor benchmarks [Ber16, ABF17a, RS16] – the smallest values ρ for small k are mostly achieved by the orthoplices. In real-world settings however, as discussed in Section 10, using the D_k lattices or the generalized m -max hash functions may lead to a better performance in practice.

Finding good spherical codes. An important open problem, both for our project-and-partition framework and for arbitrary hash families for the angular distance, is to find (if they exist) other spherical codes which achieve an even better performance than the family of orthoplices. Numerics in Section 9 suggest that as k increases, the code size c should increase faster than the scaling of $c = 2k$ offered by orthoplices. Finding the optimal scaling of c as a function of k , and finding nicer spherical codes with the appropriate scaling of c is left for future work.

Faster projections. To make e.g. hyperplane and cross-polytope hashing more practical, various ideas were proposed in e.g. [Ach01, AIL⁺15] to work with sparse projections and pseudorandom rotation matrices. Similar ideas can be used for any hash family, to reduce the cost of multiplication by a random Gaussian matrix \mathbf{A} ; replacing it with a sparse, “sufficiently random” pseudorandom matrix \mathbf{A} may be sufficient to achieve good query exponents ρ . Depending on how the pseudorandom projections are instantiated, this may lead to a different practical evaluation than what we described in Section 10.

Using orthogonal projection matrices. In our framework, we focused on projecting down onto a low-dimensional subspace using Gaussian matrices $\mathbf{A} \sim \mathcal{N}(0, 1)^{k \times d}$. For $k \ll d$, using Gaussian matrices or orthogonal matrices (i.e. $\mathbf{A}\mathbf{A}^T = I_k$) is essentially equivalent [DF87, Jia06], but for large k it may be beneficial to use proper rotations induced by orthogonal matrices. For instance, Laarhoven [Laa17] showed that for hypercube hashing in the ambient space, there is a clear gap between using random or orthogonal matrices; using orthogonal matrices generally works better.

The main issue when analyzing the same framework outlined above with orthogonal matrices is that the dependence on d then does not disappear; the distribution of \mathbf{A} then clearly relies on both k and d . Our framework is dimensionless, as the performance can be computed without knowledge of d , and for $k = 2$ this even allows us to obtain explicit expressions for the collision probabilities. Using orthogonal matrices, the collision probabilities will likely become complicated functions of d , and comparing different spherical codes may then become a difficult task. We leave it as an open problem to adjust the above framework to the setting where \mathbf{A} is orthogonal, and to see how much can be gained (in theory and in practice) by using orthogonal rather than Gaussian matrices..

Acknowledgments.

The author is supported by a Veni grant from NWO under project number 016.Veni.192.005.

References

- ABF17a. Martin Aumüller, Erik Bernhardsson, and Alexander Faithfull. ANN benchmarks – available online at <http://sss.projects.itu.dk/ann-benchmarks/>, 2017.
- ABF17b. Martin Aumüller, Erik Bernhardsson, and Alexander Faithfull. ANN-benchmarks: A benchmarking tool for approximate nearest neighbor algorithms. In *SISAP*, pages 34–49, 2017.
- Ach01. Dimitris Achlioptas. Database-friendly random projections. In *PODS*, pages 274–281, 2001.
- AI06. Alexandr Andoni and Piotr Indyk. Near-optimal hashing algorithms for approximate nearest neighbor in high dimensions. In *FOCS*, pages 459–468, 2006.
- AIL⁺15. Alexandr Andoni, Piotr Indyk, Thijs Laarhoven, Ilya Razenshteyn, and Ludwig Schmidt. Practical and optimal LSH for angular distance. In *NIPS*, pages 1225–1233, 2015.
- AINR14. Alexandr Andoni, Piotr Indyk, Huy Lê Nguyễn, and Ilya Razenshteyn. Beyond locality-sensitive hashing. In *SODA*, pages 1018–1028, 2014.
- ALRW17. Alexandr Andoni, Thijs Laarhoven, Ilya Razenshteyn, and Erik Waingarten. Optimal hashing-based time-space trade-offs for approximate near neighbors. In *SODA*, pages 47–66, 2017.
- AR15. Alexandr Andoni and Ilya Razenshteyn. Optimal data-dependent hashing for approximate near neighbors. In *STOC*, pages 793–801, 2015.
- AR16. Alexandr Andoni and Ilya Razenshteyn. Tight lower bounds for data-dependent locality-sensitive hashing. In *SOCCG*, pages 1–15, 2016.
- BDGL16. Anja Becker, Léo Ducas, Nicolas Gama, and Thijs Laarhoven. New directions in nearest neighbor searching with applications to lattice sieving. In *SODA*, pages 10–24, 2016.
- Ber16. Erik Bernhardsson. ANN benchmarks – available online at <https://github.com/erikbern/ann-benchmarks>, 2016.
- Bis06. Christopher M. Bishop. *Pattern Recognition and Machine Learning*. Springer-Verlag, 2006.
- BL16. Anja Becker and Thijs Laarhoven. Efficient (ideal) lattice sieving using cross-polytope LSH. In *AFRICACRYPT*, pages 3–23, 2016.
- Bro02. Andries E. Brouwer. Lattices - <https://www.win.tue.nl/~aeb/latt/lattices.pdf>, 2002.
- CDGG18. Karthekeyan Chandrasekaran, Daniel Dadush, Venkata Gandikota, and Elena Grigorescu. Lattice-based locality sensitive hashing is optimal. In *ITCS*, 2018.
- Cha02. Moses S. Charikar. Similarity estimation techniques from rounding algorithms. In *STOC*, pages 380–388, 2002.
- Che68. M.C. Cheng. The clipping loss in correlation detectors for arbitrary input signal-to-noise ratios. *IEEE Transactions on Information Theory*, 14(3):3, 1968.
- Che69. M.C. Cheng. The orthant probabilities of four Gaussian variables. *The Annals of Mathematical Statistics*, 40(1):152–161, 1969.
- Chr17. Tobias Christiani. A framework for similarity search with space-time tradeoffs using locality-sensitive filtering. In *SODA*, pages 31–46, 2017.
- DF87. Persi Diaconis and David Freedman. A dozen de Finetti-style results in search of a theory. *Annales de l’IHP Probabilités et statistiques*, 23(2):397–423, 1987.
- DHS00. Richard O. Duda, Peter E. Hart, and David G. Stork. *Pattern Classification (2nd Edition)*. Wiley, 2000.
- Dub10. Moshe Dubiner. Bucketing coding and information theory for the statistical high-dimensional nearest-neighbor problem. *IEEE Transactions on Information Theory*, 56(8):4166–4179, Aug 2010.
- ER08. Kave Eshghi and Shyamsundar Rajaram. Locality sensitive hash functions based on concomitant rank order statistics. In *KDD*, pages 221–229, 2008.
- GBM⁺19. Alan Genz, Frank Bretz, Tetsuhisa Miwa, Xuefei Mi, Friedrich Leisch, Fabian Scheipl, and Torsten Hothorn. *mvtnorm: Multivariate normal and t distributions*, 2019. R package version 1.0-10.
- IM98. Piotr Indyk and Rameev Motwani. Approximate nearest neighbors: Towards removing the curse of dimensionality. In *STOC*, pages 604–613, 1998.
- Jia06. Tiefeng Jiang. How many entries of a typical orthogonal matrix can be approximated by independent normals? *The Annals of Probability*, 34(4):1497–1529, 2006.
- KW17. Christopher Kennedy and Rachel Ward. Fast cross-polytope locality-sensitive hashing. In *ITCS*, pages 1–16, 2017.
- Laa15. Thijs Laarhoven. Sieving for shortest vectors in lattices using angular locality-sensitive hashing. In *CRYPTO*, pages 3–22, 2015.

- Laa17. Thijs Laarhoven. Hypercube LSH for approximate near neighbors. In *MFCS*, pages 1–20, 2017.
- Laa19. Thijs Laarhoven. MathOverflow: Normal multivariate orthant probabilities – <https://mathoverflow.net/questions/334212/normal-multivariate-orthant-probabilities>, 2019.
- LK14. Yongjae Lee and Woo Chang Kim. Concise formulas for the surface area of the intersection of two hyperspherical caps. *KAIST Technical Report*, 2014.
- MLB15. Artur Mariano, Thijs Laarhoven, and Christian Bischof. Parallel (probable) lock-free HashSieve: a practical sieving algorithm for the SVP. In *ICPP*, pages 590–599, 2015.
- MLB17. Artur Mariano, Thijs Laarhoven, and Christian Bischof. A parallel variant of LDSieve for the SVP on lattices. In *PDP*, pages 23–30, 2017.
- MO15. Alexander May and Ilya Ozerov. On computing nearest neighbors with applications to decoding of binary linear codes. In *EUROCRYPT*, pages 203–228, 2015.
- Pla54. R.L. Plackett. A reduction formula for normal multivariate integrals. *Biometrika*, 41(3–4):351–360, 1954.
- RS16. Ilya Razenshteyn and Ludwig Schmidt. FALCONN – available online at <https://falconn-lib.org/>, 2016.
- SDI05. Gregory Shakhnarovich, Trevor Darrell, and Piotr Indyk. *Nearest-Neighbor Methods in Learning and Vision: Theory and Practice*. MIT Press, 2005.
- Sha59. Claude E. Shannon. Probability of error for optimal codes in a Gaussian channel. *Bell System Technical Journal*, 38(3):611–656, 1959.
- She99. William F. Sheppard. On the application of the theory of error to cases of normal distribution and normal correlation. *Philosophical Transactions of the Royal Society A*, 192:101–167, 1899.
- Slo. Neil J.A. Sloane. Spherical codes: nice arrangements of points on a sphere in various dimensions.
- Ste62. G.P. Steck. Orthant probabilities for the equicorrelated multivariate normal distribution. *Biometrika*, 49(3–4):433–445, 1962.
- TT07. Kengo Terasawa and Yuzuru Tanaka. Spherical LSH for approximate nearest neighbor search on unit hypersphere. In *WADS*, pages 27–38, 2007.
- TT09. Kengo Terasawa and Yuzuru Tanaka. Approximate nearest neighbor search for a dataset of normalized vectors. In *IEICE Transactions on Information and Systems*, volume 92, pages 1609–1619, 2009.